CO₂ Capture by Absorption with Potassium Carbonate

Authors: Gary T. Rochelle, Eric Chen, J. Tim Cullinane,
Marcus Hilliard, Jennifer Lu, Babatunde Oyenekan, and Ross Dugas

Disclaimer

This report was prepared as an account of work sponsored by an agency of the United States Government. Neither the United States Government nor any agency thereof, nor any of their employees, makes any warranty, express or implied, or assumes any legal liability or responsibility for the accuracy, completeness, or usefulness of any information, apparatus, product, or process disclosed, or represents that its use would not infringe privately owned rights. Reference herein to any specific commercial product, process, or service by trade name, trademark, manufacturer, or otherwise does not necessarily constitute or imply its endorsement, recommendation, or favoring by the United States Government or any agency thereof. The views and opinions of authors expressed herein do not necessarily state or reflect those of the United States Government or any agency thereof.

Abstract

The objective of this work is to improve the process for CO_2 capture by alkanolamine absorption/stripping by developing an alternative solvent, aqueous K_2CO_3 promoted by piperazine. CO_2 mass transfer rates are second order in piperazine concentration and increase with ionic strength. Modeling of stripper performance suggests that 5 m K^+/2.5 m PZ will require 25 to 46% less heat than 7 m MEA. The first pilot plant campaign was completed on June 24. The CO_2 penetration through the absorber with 20 feet of Flexipac™ 1Y varied from 0.6 to 16% as the inlet CO_2 varied from 3 to 12% CO_2 and the gas rate varied from 0.5 to 3 kg/m^2-s.

Contents

Contents

Figures

Tables

Introduction

The objective of this work is to improve the process for CO_2 capture by alkanolamine absorption/stripping by developing an alternative solvent, aqueous K_2CO_3 promoted by piperazine. This work expands on parallel bench scale work with system modeling and pilot plant measurements to demonstrate and quantify the solvent process concepts.

The bench-scale and modeling work is supervised by Gary Rochelle. Frank Seibert is supervising the pilot plant. Two graduate students (Babatunde Oyenekan, Ross Dugas) have received support during this quarter for direct effort on the scope of this contract. Five students supported by other funding have made contributions this quarter to the scope of this project (Eric Chen – EPA Star Fellowship; Tim Cullinane, Jennifer Lu, Marcus Hilliard – Various Industrial Sponsors; Ross Dugas – Teaching Assistant).

Experimental

The following sections of this report detail experimental methods:

Subtask 1.2 describes the wetted wall column used for CO_2 rate measurements.

Subtask 2.1d describes a method of acid/base titration for determination of total alkalinity and piperazine.

Subtask 2.3 details the final modifications made on the pilot plant.

Subtask 2.4 describes the methods used in the pilot plant for the first campaign.

Results and Discussion

Progress has been made on five subtasks in this quarter:

Subtask 1.1 – Modify Vapor-Liquid Equilibrium (VLE) Model

A manuscript has been prepared on the completed work to represent the $K_2CO_3/PZ/CO_2/H_2O$ with the stand-alone electrolyte NRTL model.

Marcus Hilliard has obtained salt/water parameters and equilibrium constants for the electrolyte NRTL model in AspenPlus to represent the available thermodynamic data for $K_2CO_3/CO_2/H_2O$ and $PZ/CO_2/H_2O$. A paper was prepared for the Seventh International Conference on Greenhouse Gas Control Technologies (GHGT-7).

Subtask 1.2 – Modify Point Rate Model

Tim Cullinane has measured CO_2 mass transfer rates in the K_2CO_3/piperazine solvent at 80 to $110^{o}C$. Preliminary analysis of these and previous rate data at $25\text{-}60^{o}C$ has shown effects of ionic strength and piperazine concentration. A paper was prepared for GHGT-7.

Subtask 1.4 – Predict Absorber/Stripper Pilot Results

Babatunde Oyenekan has predicted the performance of the pilot plant stripper for 7 m MEA and 5 m K^+ / 2.5 m PZ with a simple spreadsheet model. A paper was prepared for GHGT-7.

Jennifer Lu has used further modification of equilibrium and rate parameters in the existing Freguia model of MEA absorption to predict the performance of 5 m K^+/2.5 m PZ and 7 m MEA in the pilot plant.

Subtask 2.1 – Pilot Plant Test Plan

Ross Dugas has developed a method of acid/base titration to determine total alkalinity and piperazine in solutions from the pilot plant.

Subtask 2.3 – Install and Modify Equipment

The pilot plant modifications were completed in late May.

Subtask 2.4 – Campaign 1

The pilot plant was operated with data collection from June16 - June 24. The final week of operations tested solvent up to 5 m K^+/2.5 m PZ. Quantitative results were obtained for absorber performance with Koch Flexipac™ 1Y.

Conclusions

1. The AspenPlus™ electrolyte NRTL describes the H_2O-K_2CO_3-CO_2 property data with an average absolute error of +/- 5.8 % and the PZ-CO_2-H_2O property data with an average absolute error of +/- 2.3 %.

2. An optimum concentration ratio of 2:1 for K^+ to PZ has been observed in rate experiments.

3. The temperature behavior demonstrated by k_g' indicates that kinetics controls the absorption process at absorber conditions. At stripper conditions, the temperature dependence is small and the process is likely controlled by the diffusion of reactants and products to and from the gas-liquid interface.

4. Preliminary modeling of the CO_2 absorption rate in aqueous PZ indicates the mechanism appears to be second order with respect to the amine.

5. Ionic strength has a significant impact on the rate constants.

6. The simple stripper model suggests that 7 m MEA requires 18 to 34% more heat than 5 m K+/2.5 m PZ when a 10°C approach is used and the stripper is operated at 160 kPa. If the CO_2 vapor pressure is always twice that of 7 m MEA, the energy savings range from 25 to 46%.

7. In all cases, for the same amount of packing, the PZ solvent gives a richer solution and a higher rich partial pressure than 7 m MEA. With 15 m of packing, the PZ solvent has a higher rich loading and a higher rich partial pressure. With 6.1 m (20 ft)

of packing, the PZ solvent achieves the same removal as the MEA solvent, with a much higher rich partial pressure, nearly 4 times greater.

8. The pilot plant operated smoothly with gas at 0.5 to 3 kg/m^2-s and L/G of 1.1 to 5.4 kg/kg. Both 3% and 12% CO_2 was achieved in the recycled gas without major continuous makeup of CO_2, so leaks were minimal.

9. With 20 feet of Flexipac™ 1Y packing the pilot absorber achieved 0.2 to 13% CO_2 penetration at 3% CO_2 and 5 to 15% penetration at 12% CO_2. These ranges of CO_2 performance correspond to gas rates from 0.5 to 3 kg/m^2-s.

10. The precipitation of solid piperazine created some manageable operating problems in the pilot plant.

11. Reasonable data on stripper performance and heat rate were not obtained because of a design mistake in the steam traps for the solvent heater.

Future Work

A revised schedule of major milestones is given here:

Revised Schedule: s = start, f = finish

Task	Month >>>	2002		2003				2004				2005		
---	---	7	10	1	4	7	10	1	4	7	10	1	4	7
1	**Modeling**													
1.1	Modify VLE model	s								f				
1.2	Modify point rate model			s							f			
1.3	Integrate and debug			s										f
1.4	Predict pilot results				s				f					
1.5	Simulate base case pilot									s	f			
1.6	Simulate & Optimize P & V_g effects									s			f	
1.7	Simulate and Optimize packing effects										s			f
1.8	Predict flowsheet options											s	f	
1.9	Economic Analysis												s	f
1.10	Simulate MEA Baseline									s			f	
2	**Pilot Plant**													
2.1	Test Plan						s	f						
2.2	Design modifications, order equipment & packing	s						f						
2.3	Install and modify equipment			s					f					
2.4	Troubleshoot, base case							s	f					
2.5	Optimize V_g and P									s	f			
2.6	Structured packing												s	f
2.7	MEA Baseline Testing											s	f	

We expect the following accomplishments in the next quarter:

Subtask 1.1 – Modify Vapor-Liquid Equilibrium (VLE) Model

The AspenPlus™ model will be regressed to represent the CO_2 solubility in 5 m K^+/2.5 m PZ.

Subtask 1.2 – Modify Point Rate Model

Parameters will be developed to represent measured absorption rates with the rigorous model of mass transfer by Bishnoi.

Subtask 1.3 – Develop Integrated Absorber/Stripper Model

Initial results will be obtained to simulate the stripper with Aspen Custom Modeler.

The existing absorber model for MEA will be modified to accept piperazine species.

Subtask 1.4 – Predict Absorber/Stripper Pilot results

The simple stripper model will be extended to multi-pressure stripper configuration to reduce steam requirements.

As the refinements to the absorber simulation are implemented, pilot plant performance will be modeled. Once the interaction parameters for MEA and K^+ and PZ and K^+ are available, they will be added to the simulation.

Subtask 2.1 – Pilot Plant Test Plan

Detailed test plans will be developed for the second and third pilot plant campaigns.

Subtask 2.5 – Campaign 2

The second campaign in the pilot plant is scheduled to begin in late September, 2005. The pilot plant will be operated for four weeks with 5 m K^+/ 2.5 m PZ. Performance data will be obtained for both the stripper and the absorber.

Task 1 – Modeling Performance of Absorption/Stripping of CO_2 with Aqueous K_2CO_3 Promoted by Piperazine

Subtask 1.1b – Modify Vapor-Liquid Equilibrium (VLE) Model – Aspen Plus™

by Marcus Hilliard
(Supported by various industrial sponsors)

Introduction

In recent years, CO_2 emissions from coal-fired power plants continue to contribute to the steady rise in global warming greenhouse gasses. A recent report from the Environment Protection Agency (2002) states that CO_2 emissions from the combustion of fossil fuels represent approximately ninety-six percent of the total CO_2 emissions produced in the United States and approximately thirty-six percent of the CO_2 emissions originate from the combustion of fossil fuels in coal-fired power plants. As a result, CO_2 capture technologies continue to become one of the most important industrial and academic research areas as concerns over the effects global warming multiply.

CO_2 removal by aqueous absorption/stripping using monoethanolamine (MEA) and other blended amine solvents has been established as a mature CO_2 capture technology. The development of new solvents involving potassium carbonate and piperazine has shown potential as a new CO_2 capture process (Cullinane, 2002).

The vision of this project expands upon previous work in the area of modeling amines and amine blends for the application of CO_2 capture via gas treating (Cullinane, 2002; Cullinane et al., 2004; Austgen, 1989; Posey, 1996; Bishnoi, 2000). By utilizing the electrolyte NRTL model (Chen et al., 1982; Chen et al., 1979) within Aspen Plus[TM], simultaneously regressed binary interaction parameters and chemical equilibrium constants were determined to describe the speciation and equilibrium behavior of potassium carbonate and piperazine solutions. Using an accurate thermodynamics package for the design and optimization of separation equipment to predict the chemical and phase equilibrium behavior within a process simulator encompasses the endeavor associated with this project.

Thermodynamic Modeling and Results

Figure 1 illustrates the proposed system to correlate/predict the solubility of carbon dioxide in aqueous solutions of potassium carbonate and piperazine.

H_2O-K_2CO_3-CO_2 System

To develop a working model of potassium carbonate/bicarbonate mixtures, electrolyte NRTL water/salt binary interaction parameters were regressed for significant contributing species. Equilibrium constants, R1-R3, were taken from Posey (1996) and Edwards et al. (1978). Through simultaneous regression, binary adjustable parameters

for the potassium carbonate/potassium bicarbonate/water electrolyte system were obtained through the regression of mean ionic activity coefficient (Aseyev et al., 1996), water vapor pressure (osmotic coefficient) (Aseyev et al., 1996; Aseyev, 1999; Sarbar et al., 1982; Roy et al., 1984) and calorimetry (heat capacity of solution) (Aseyev et al., 1996) over potassium carbonate and potassium bicarbonate solutions and CO_2 solubility in potassium carbonate (Tosh et al., 1959). The data provide a wide range of both temperature and concentration but were reduced (excluding the CO_2 solubility data) to cover the range in temperature and concentration from 298 to 403 K and 14 to 36 weight percent (wt%) K_2CO_3, respectfully, to describe absorber/stripper conditions. Potassium carbonate and potassium bicarbonate were assumed to completely dissociate in an aqueous solution.

$$Vapor\ Phase$$
$$CO_2 \qquad H_2O$$

$$CO_2 \qquad H_2O \qquad Liquid\ Phase$$

$R1 \qquad 2H_2O \rightleftharpoons H_3O^+ + OH^-$

$R2 \qquad CO_2 + 2H_2O \rightleftharpoons H_3O^+ + HCO_3^-$

$R3 \qquad HCO_3^- + H_2O \rightleftharpoons H_3O^+ + CO_3^{-2}$

$R4 \qquad PZH^+ + H_2O \rightleftharpoons PZ(l) + H_3O^+$

$R5 \qquad PZ(l) + HCO_3^- \rightleftharpoons PZCOO^- + H_2O$

$R6 \qquad PZCOO^- + HCO_3^- \rightleftharpoons PZ\left(COO^-\right)_2 + H_2O$

$R7 \qquad H^+PZCOO^- + PZ(l) \rightleftharpoons PZCOO^- + PZH^+$
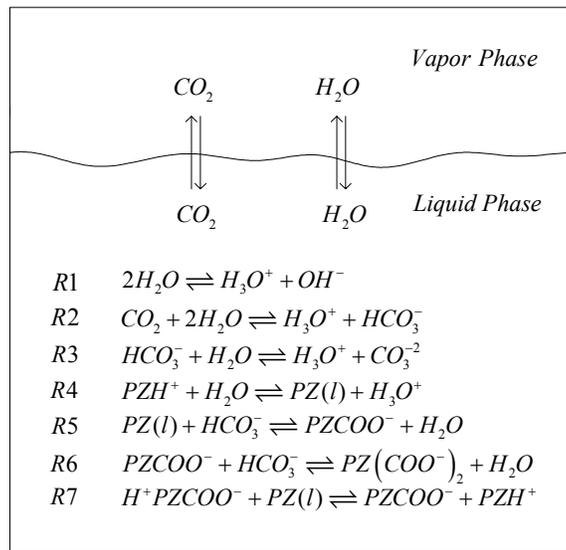
Figure 1. Chemical and Vapor-Liquid Equilibrium of K_2CO_3 and PZ

Adjustable binary interaction parameters were determined by the Data Regression System[TM] (DRS) within Aspen Plus[TM] using the maximum likelihood principle of Britt and Luecke (1973). The objective function is then minimized through the use of Lagrange multipliers to adjust the measurable variables and the model parameters within vapor-liquid equilibrium constraints and parameter bounds. With the determination of the estimates for the binary interaction parameters known for the model, a simple Aspen Plus[TM] Flash model was used to test the predictive capability of the H_2O-K_2CO_3- CO_2 model against literature data. Table 1 gives the absolute percent relative error for the model predictions.

Table 1. Overall Simultaneous Regression

H$_2$O/K$_2$CO$_3$ System	Ave. % Deviation	Max. % Deviation
Percent Relative Error:		
Vapor Pressure Depression*	11.9	27.2
Heat Capacity of Solution	1.5	4.5
Mean Ionic Activity Coefficient	2.5	4.8
H$_2$O/KHCO$_3$ System		
Vapor Pressure Depression*	0.9	6.2
Heat Capacity of Solution	1.1	3.4
CO$_2$ Solubility		
20 wt%	14	36.2
30 wt%	13	37.5
40 wt%	14	51.7
Overall Percent Relative Error	5.8	51.7

*Based osmotic coefficient data

CO$_2$ solubility data ranges from 343 -403 K

Overall, the model adequately describes the H$_2$O-K$_2$CO$_3$-CO$_2$ property data listed above within an average absolute error of +/- 5.8 percent, with the exception of a few outliers.

We found that parameters sequentially regressed for the above two systems without CO$_2$ solubility data (Tosh et al., 1959) did not accurately describe significant systematic trends presented in the vapor-liquid equilibrium. Sequential regression consists of a two-part process where parameters for the H$_2$O-K$_2$CO$_3$ system were determined and then held fixed while parameters for the H$_2$O-KHCO$_3$ system were regressed. Model predictions gave an average absolute error of +/- 250 percent for the predicted/experimental partial pressure of CO$_2$ from 20 – 40 equivalent wt% K$_2$CO$_3$ versus temperature from 343 – 493 K.

H$_2$O-PZ System

To develop a working model for aqueous piperazine mixtures, NRTL (Renon et al., 1968) molecule/molecule binary interaction parameters for H$_2$O-PZ were regressed from activity coefficient predictions by UNIFAC (Gmehling et al., 1993). The activity coefficient data included the range in temperature from 298 to 323 K and composition from 0.1 to 3 moles of PZ per kg of H$_2$O. The equilibrium constant, R4, was taken from Hetzer et al. (1968) and corrected for the symmetric reference state for the activity coefficient of piperazine from infinite dilution in water to infinite dilution in amine solvent. Table 2 gives the absolute percent relative error for the model predictions.

Table 2. Overall Regression Results

H2O/PZ System	Ave. % Deviation	Max % Deviation
Percent Relative Error		
Activity Coefficient Data for Piperazine as f(T)		
Temp. (K)		
298	3.0	6.1
303	1.7	4.9
308	1.2	3.5
313	1.0	4.4
318	1.3	4.7
323	2.2	4.3
Overall Percent Relative Error	1.7	6.1

Overall, the model adequately describes the PZ-H_2O UNIFAC activity coefficient data within an average absolute error of +/- 1.7 percent, with the exception of a few outliers.

H_2O-PZ-CO_2 System

Development of a working model for piperazine/carbon dioxide mixtures, electrolyte NRTL water/salt and molecule/molecule interaction parameters were regressed for significant contributing species. Equilibrium constants, R5-R7, were taken from Cullinane et al. (2004). Equilibrium reactions R5 and R6 were transformed to remove the floating carbon dioxide concentration dependence incorporated into the Aspen Plus^{TM} electrolyte NRTL code. Equilibrium reaction, R7, was also transformed to represent significant contributing species as described by speciation predictions for the solubility of carbon dioxide in 0.6 moles per liter (M) of aqueous piperazine from Bishnoi (2000). Through simultaneous regression, binary adjustable parameters were obtained through the regression of total pressure (Kamps et al., 2003) and CO_2 solubility in piperazine (Bishnoi, 2000) data. The data included the range in temperature and concentration from 313 to 393 K and 2 to 4 mole PZ/kg of H_2O, respectively. Including this data was necessary to describe the chemical equilibrium reaction of protonated piperazine carbamate to piperazine carbamate plus protonated piperazine.

Overall, the model adequately describes the PZ-CO_2-H_2O property data listed above within an average absolute error of +/- 2.3 percent, with the exception of a few outliers. As can be seen from Figure 2, model predictions for the partial pressure of carbon dioxide agree well with the experimental results with an average absolute error of +/- 17.5 percent. Using the model as a predictive tool, the model describes similar systematic trends for the partial pressure of carbon dioxide at 298 and 373 K as predicted by Cullinane et al. (2004).
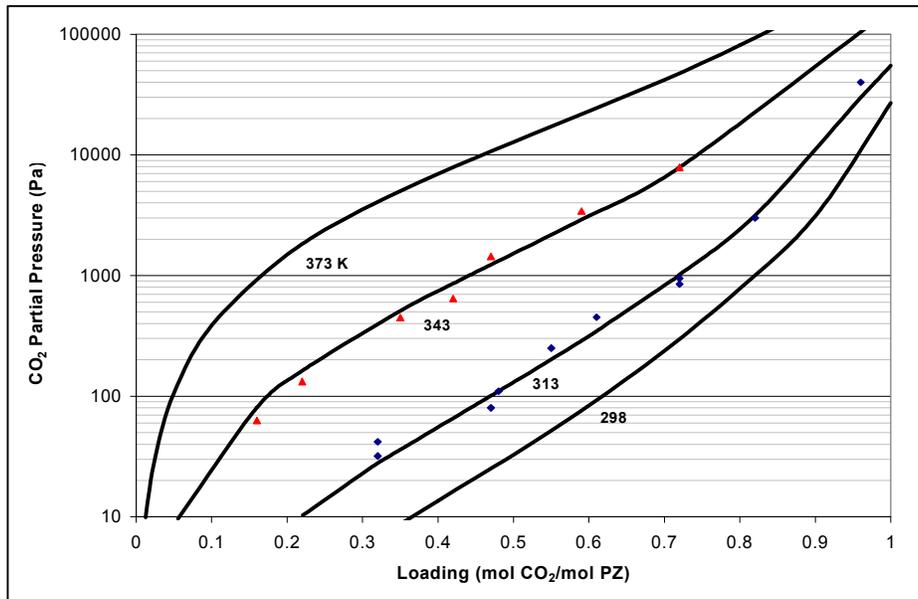
**Figure 2. CO$_2$ Partial Pressure in 0.6 M Piperazine. Points: Experimental [5]. Lines: Model Predictions. (Aspen Regressed Parameters)**

Future Work

Piperazine speciation from Ermatchkov et al. (2003) for the H$_2$O-PZ-CO$_2$ system and proton NMR and CO$_2$ solubility (Cullinane et al., 2004) data for the mixed solvent system of H$_2$O-PZ-K$_2$CO$_3$ will then be regressed to finish the thermodynamic modeling framework.

Subtask 1.2 – Modify Point Rate Model

by J. Tim Cullinane
(Supported by various industrial sponsors)

Introduction

This report presents the continuing development of aqueous potassium carbonate-piperazine mixtures for CO_2 removal from flue gas. Previous reports present a rigorous thermodynamic model, developed and verified with VLE and speciation in aqueous K^+/PZ. Equilibrium constants have been regressed and solution behavior has been analyzed.

The rate of CO_2 absorption was collected simultaneously with the previous VLE measurements and interpreted as a normalized flux. This paper reports preliminary efforts to model the rate of CO_2 absorption and explain observed absorption behavior.

The rate performance of concentrated K^+/PZ mixtures are shown to be 1.5 to 5 times that of MEA. A strong effect of temperature is observed at absorber conditions (40 to 80°C), but not at stripper conditions (100 to 110°C). An optimum concentration ratio of K^+ to PZ is observed experimentally and explained with model predictions of speciation. The mechanism of CO_2 absorption is shown to be second order with PZ, and rate constants are interpreted. Ionic strength appears to plays a significant role in determining the overall absorption rate.

Experimental

As with the P_{CO2}* measurements reported previously, a wetted-wall column, shown in a flowsheet in Figure 3, was used to measure CO_2 absorption rates in various solvents. The column is a stainless-steel tube, measuring 9.1 cm in height and 1.26 cm in diameter (38.5 cm^2 total area based on the liquid film). The gas-liquid contact region is enclosed by a 2.54 cm OD thick-walled glass tube. A circulating bath of oil, enclosed by a 10.16 cm OD glass annulus, insulates the column from ambient conditions.

The chemical solvent was contained in a 1000 mL reservoir. A pump pushes the solution through a coil in a heated circulator at a flowrate between 2 and 4 cm^3/s. The solution is then pumped through the inside of the wetted-wall column, contacting the gas stream. The liquid is collected and pumped back to a liquid reservoir.

Nitrogen and carbon dioxide flowrates are controlled with Brooks mass flow controllers; the total flowrate is maintained between 4 and 6 L/min. CO_2 partial pressures are controlled between 10 to 30,000 Pa. The gases are mixed and saturated with water in a 400 mL reservoir heated in an oil bath. The gas flows through the gas-liquid contact region and absorbs or desorbs CO_2. After exiting the column, the gas is dried in a condenser and a drying column. The outlet CO_2 concentration is measured using a carbon dioxide analyzer.
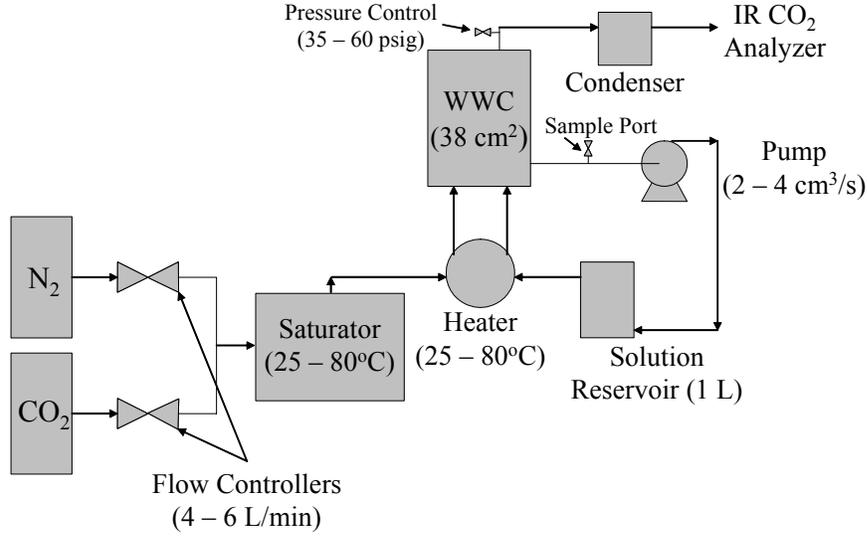
Figure 3. Flowsheet of the Wetted-Wall Column

Data collected from the wetted-wall column is analyzed by interpreting the flux as a normalized flux, kg', defined as

$$N_{CO_2} = k_g' \left(P_{CO_2,i} - P_{CO_2}^* \right)$$

(1)

This mass transfer coefficient represents the liquid film resistance, including kinetic contributions, in the form

$$N_{CO_2} = \frac{\sqrt{D_{CO_2} k_{Am} [Am]_i}}{H_{CO_2}} \left(P_{CO_2,i} - P_{CO_2}^* \right)$$

(2)

where $[Am]_i$ represents the amine concentration at the gas-liquid interface, k_{Am} is the pseudo-first order rate constant, D_{CO_2} is the diffusion coefficient of CO_2, and H_{CO_2} is the Henry's constant of CO_2. From experiments, the normalized flux was calculated from the following expression.

$$k_g' = \left(\frac{1}{K_G} - \frac{1}{k_g} \right)^{-1}$$

(3)

K_G is an overall gas transfer coefficient defined as

$$N_{CO_2} = K_G \left(P_{CO_2,b} - P_{CO_2}^* \right)$$

(4)

An equilibrium partial pressure, P_{CO2}^*, was determined for each experiment by collecting data at various bulk partial pressures, near equilibrium, so that P_{CO2}^* could be found by interpolating to a flux of 0.0. K_G is calculated as the slope of the flux versus the log mean pressure, ΔP_{lm}. The ΔP_{lm} is defined as a log mean difference in bulk gas partial pressures of CO_2 across the column.

$$\Delta P_{lm} = \frac{P_{CO_2,in} - P_{CO_2,out}}{\ln\left(P_{CO_2,in}/P_{CO_2,out}\right)} \tag{5}$$

A demonstration of finding $P_{CO2}*$ and K_G is shown in Figure 4.
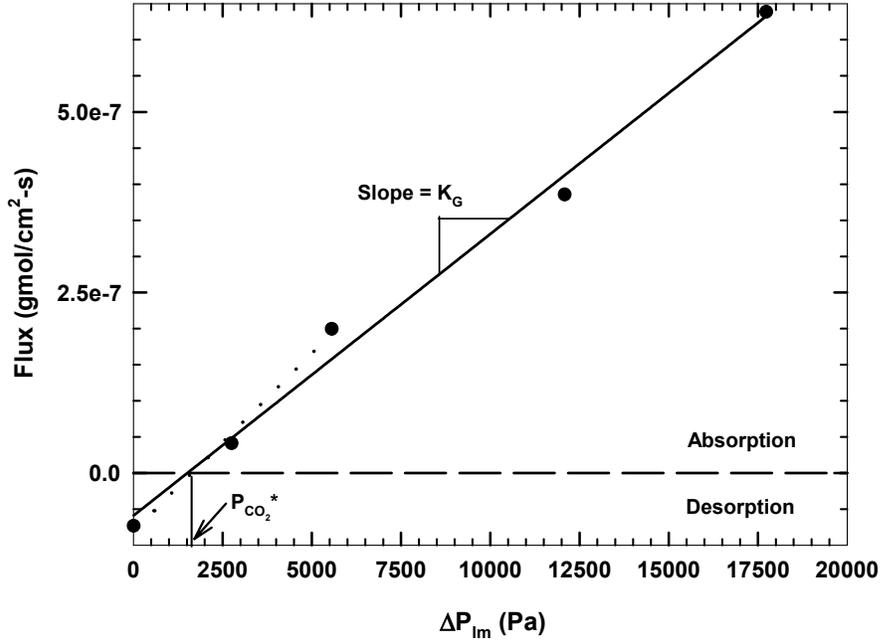
Figure 4. Determination of $P_{CO2}*$ and K_G for 3.6 m K$^+$/0.6 m PZ at 40°C and α = 0.221

The gas phase mass transfer coefficient, k_g, for the wetted-wall column was calculated using a correlation determined by Pacheco (1998).

$$Sh = 1.075\left(Re\,Sc\,\frac{d}{h}\right)^{0.85} \tag{6}$$

where Re is the Reynolds number, Sc is the Schmidt number, d is the hydraulic diameter of the column, and h is the height of the column. The Sherwood number, Sh, yields k_g from

$$Sh = \frac{RTk_g h}{D_{CO_2}} \tag{7}$$

where R is the gas constant and T is temperature. The diffusion coefficient was assumed to be that of CO_2 in water and was calculated by the expression given in Versteeg and van Swaaij (1988).

$$D_{CO_2}\left(m^2/s\right) = 2.35\times10^{-6}\exp\left(\frac{-2119}{T(K)}\right) \tag{8}$$

A rate model has been developed to predict the flux of CO_2 into amine solvents (Bishnoi, 2000). This work has modified the model to include PZ and K^+. The model uses the eddy diffusivity theory, shown in Equation (9) with a pseudo-first order assumption in the reaction term, for modeling the boundary layer. Further details concerning the solution to this equation can be found in Glasscock (1990).

$$\frac{\partial}{\partial x}\left[\left(D_{CO_2} + \varepsilon x^2\right)\frac{\partial[CO_2]}{\partial x}\right] - k_1[CO_2] = 0 \tag{9}$$

The rate model integrates the differential equation using multiple nodes across a dimensionless boundary layer. The model requires an estimation of the diffusion coefficient of reactants and products, but accounts rigorously for gas phase resistance, liquid phase resistance, equilibrium, and kinetic contributions.

The model predicts a flux by using a bulk, gas-phase partial pressure of CO_2 and the bulk solution composition as found by the equilibrium model. The model iteratively solves for an interface partial pressure until a continuous solution is obtained, satisfying the gas film and liquid film resistances. With the use of a non-linear regression package, GREG (Caracotsios, 1986) rate constants were adjusted so that a minimum in the least squares error was obtained.

The reaction mechanism of CO_2 absorption into water consists of the conversion of carbonate to bicarbonate. The controlling mechanism, however, is generally given as a reaction of CO_2 with a hydroxyl ion to give a bicarbonate ion.

$$CO_2 + OH^- \longleftrightarrow HCO_3^- \tag{10}$$

The rate is well defined and can be predicted using a second order rate constant that is proportional to the hydroxyl concentration and corrected for ionic strength (Astarita et al., 1983).

$$\log k_{OH} = 13.635 - 2895/T + 0.08I \tag{11}$$

The reversible rate, defined in terms of concentrations and the defined equilibrium constants, is

$$r = k_{OH^-}\left(\left[OH^-\right]\left[CO_2\right] - \frac{K_{HCO_3^-}}{K_w}\left[HCO_3^-\right]\right) \tag{12}$$

This rate is considerably slower than the reaction of CO_2 with amines and plays only a minor role in defining CO_2 absorption in amine-based solvents.

The accepted mechanism of amines reacting with CO_2, the zwitterion mechanism, was proposed by Caplow (1963). In this mechanism, the CO_2 and the amine form a zwitterion intermediate [Equation (13)]. Following formation, the intermediate can be deprotonated by a base, such as the free amine [Equation (14)] or water.

$$\tag{13}$$

$$(14)$$
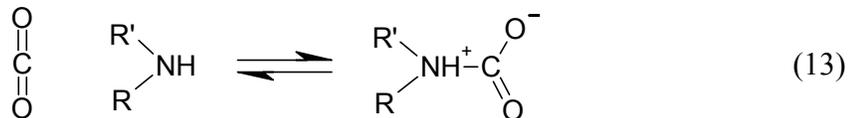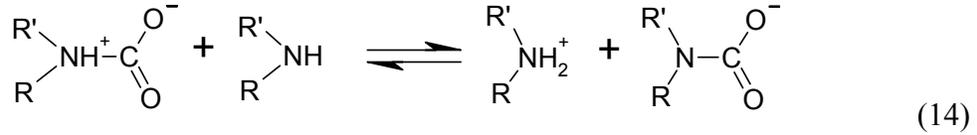
With this mechanism, the kinetic expression is

$$r = \frac{k_f [CO_2][Am]}{1 + \dfrac{k_r}{\sum k_b [B]}}$$

$$(15)$$

Thus, when the formation of the intermediate is the rate controlling step, the contribution of the bases, $\sum k_b[B]$, is large and the denominator reduces to a value of one. When deprotonation of the intermediate is rate controlling, $\sum k_b[B]$ is small so that the denominator must be considered.

In this work, the forward rate of PZ reacting with CO_2 was represented as a zwitterion mechanism in which PZ and water are the acting bases for proton extraction. This leads to the following expansion of Equation (15).

$$r = \frac{k_f [CO_2][PZ]}{1 + \dfrac{k_r}{k_{b,PZ}[PZ] + k_{b,H_2O}}}$$

$$(16)$$

where $k_{b,PZ}$ represents the extraction of protons from PZ by itself and $k_{b,H2O}$ represent a pseudo-zero order rate constant associated with the extraction of protons by water. This expression can be further simplified by assuming the 1 in the denominator is negligible compared to the contribution of the bases and by combining the rate constants. With this simplification, the reversible rate for PZ reacting with CO_2 can be written

$$r = \left(k_{PZ-PZ}[PZ] + k_{PZ-H_2O}\right)\left([PZ][CO_2] - \frac{K_W}{K_{PZCOO^-}}\frac{[PZCOO^-]}{[OH^-]}\right)$$

$$(17)$$

A similar rate expression can be derived for $PZCOO^-$.

In addition to the rigorous rate model, the data was analyzed with the common pseudo-first order assumption. Many times, amine reactions can be considered first order in CO_2 concentration and first order in amine concentration. Under normal conditions, the amine is at a nearly constant concentration across the boundary layer and the reaction rate can be represented by a pseudo-first order rate constant, k_1, and the concentration of CO_2 as in Equation (9). Under these conditions, the solution for the flux is

$$N_{CO_2} = \frac{\sqrt{D_{CO_2} k_{Am}[Am]_b}}{H_{CO_2}}\left(P_{CO_2,i} - P_{CO_2}^*\right)$$

$$(18)$$

where the pseudo-first order rate constant is replaced by a rate constant, k_{Am}, and the concentration of the amine in the bulk solution, $[Am]_b$. $P_{CO2,i}$ and $P_{CO2}*$ represent the partial pressure of CO_2 at the interface and the equilibrium partial pressure of CO_2 in the bulk solution, respectively.

Results and Discussion

Rate data collected on various solvents is presented in Figure 5 as a normalized flux. Each reported value is an average of four to seven individual points at a constant loading, but at different bulk gas compositions. A solution containing "catalytic" amounts of PZ (0.6 m) provides a rate 50% lower than those observed in 5.0 M MEA. Concentrated mixtures (5.0 m K^+/2.5 m PZ or 3.6 m K^+/1.8 m PZ) give rates 1.5 to 5 times that of MEA.
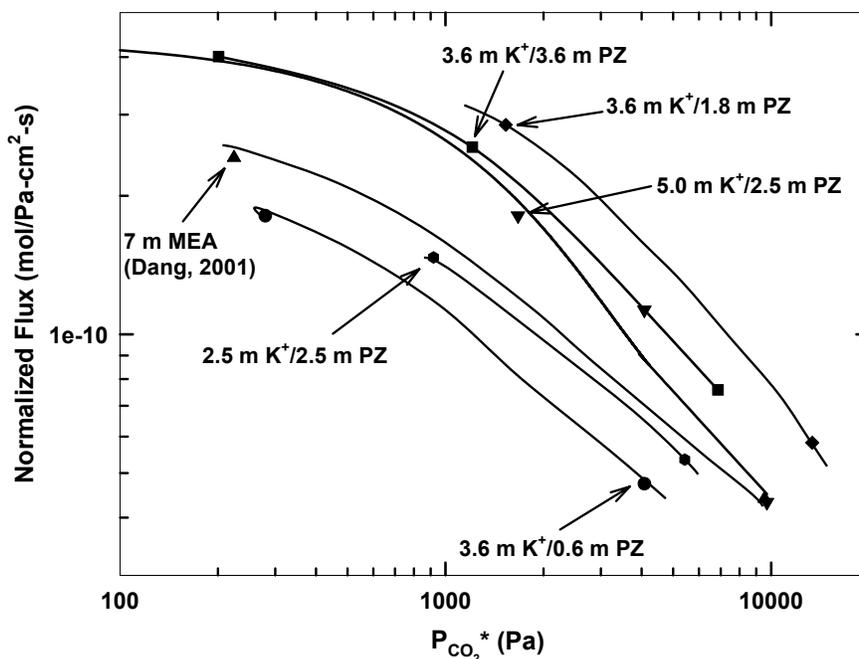
Figure 5. CO_2 Absorption Rate in K^+/PZ at 60°C

The ratio of K^+ to PZ, not just PZ concentration, has an effect on rate. This behavior is observed experimentally in Figure 5 and can be explained by speciation. Figure 6 shows the amount of reactive PZ predicted by the electrolyte NRTL model. With a constant PZ concentration, the model predicts that K^+/PZ = 2 will maximize the fraction of PZ present as reactive species. With a constant K^+ concentration, the model suggests maximizing PZ concentration in the solvent. In terms of rate performance, the PZ concentration should be maximized given that two times that of K^+ can be added within the given solubility limits. This behavior is observed at both low and high loadings (P_{CO2}* = 300 and 3000 Pa). A manuscript discussing this topic and the construct of the ENRTL model in greater detail is in preparation (Cullinane, 2004).

Figure 7 shows the dependence of rate on temperature at constant CO_2 partial pressures. Between 40 and 80°C, the rate increases with temperature. At 80 to 110°C, the temperature seems to have little effect on rate. This suggests that at higher temperatures, the mechanism of CO_2 absorption shifts from one limited by kinetics to one limited by the diffusion of reactants and products in the liquid film.
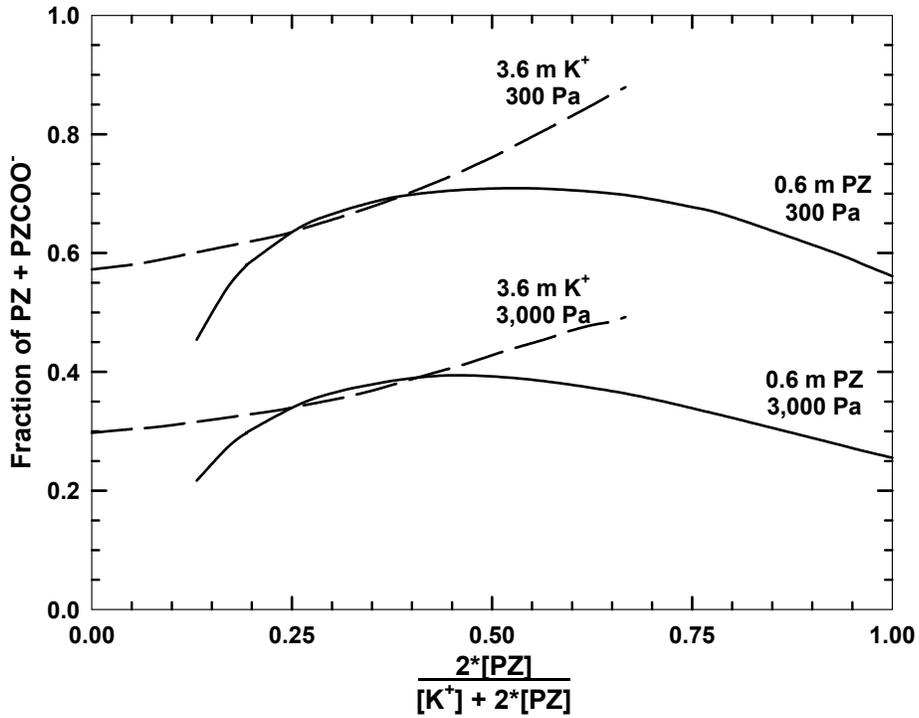
Figure 6. Optimum K^+/PZ Ratio at 60^oC Predicted by ENRTL Model at $P_{CO2}^* = 300$ and 3000 Pa (Cullinane, 2004)
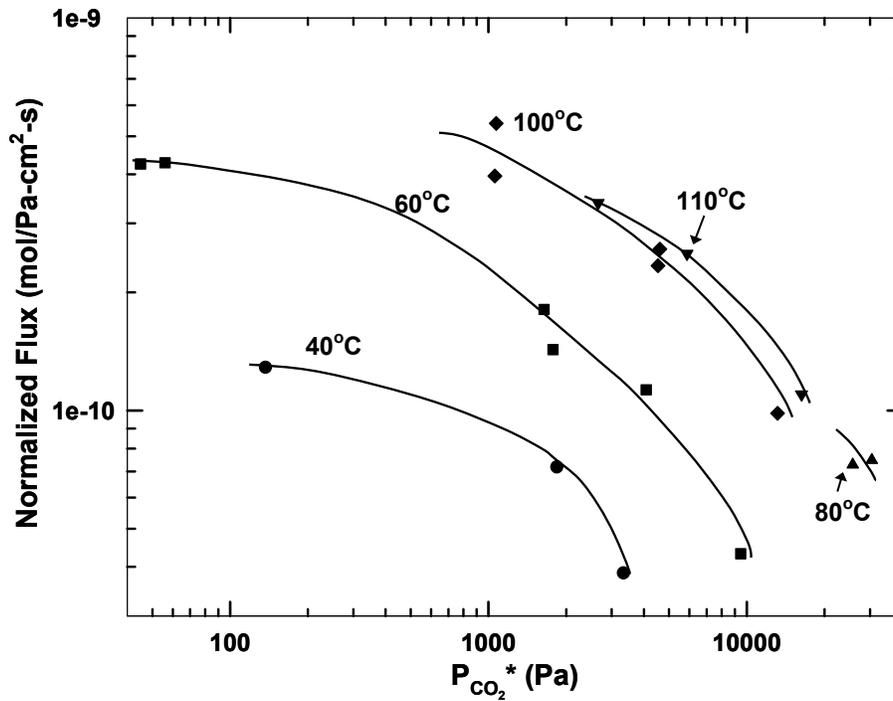
Figure 7. CO_2 Absorption Rate in 5.0 m K^+/2.5 m PZ

To quantify the reaction mechanism and kinetics of CO_2 absorption by PZ, experiments on unloaded solutions were performed at low driving force conditions for 0.2 to 1.3 M PZ. Some data was initially interpreted by Bishnoi (2000) assuming the reaction is pseudo-first order with respect to CO_2.

$$N_{CO_2} = \frac{\sqrt{D_{CO_2} k_2 [PZ]}}{H_{CO_2}} P_{CO_2} \tag{19}$$

P_{CO2} is the CO_2 partial pressure in the bulk gas. As Figure 8 shows, new data suggests that this representation leads to a linear dependence of k_2 on PZ concentration, inferring a more complicated reaction mechanism. Within the proposed "zwitterion" mechanism and recognizing the significant bases in solution, k_2 can be represented as

$$k_2 = k_{PZ-PZ}[PZ] + k_{PZ-H_2O}[H_2O] = k_{PZ-PZ}[PZ] + k'_{PZ-H_2O} \tag{20}$$

where k_{PZ-PZ} and k_{PZ-H2O} are third order rate constants and k_{PZ-H2O}' is a pseudo-second order rate constant. The total flux may then be expressed as

$$N_{CO_2} = \frac{\sqrt{D_{CO_2}\left(k_{PZ-PZ}[PZ]^2 + k'_{PZ-H_2O}[PZ]\right)}}{H_{CO_2}} P_{CO_2} \tag{21}$$

and the rate constants are interpreted to be

$$k_{PZ-PZ} = 4.04 \times 10^4 \left(\frac{m^6}{kmol^2 - s}\right) \text{ and } k'_{PZ-H_2O} = 3.62 \times 10^4 \left(\frac{m^3}{kmol - s}\right) \tag{22}$$
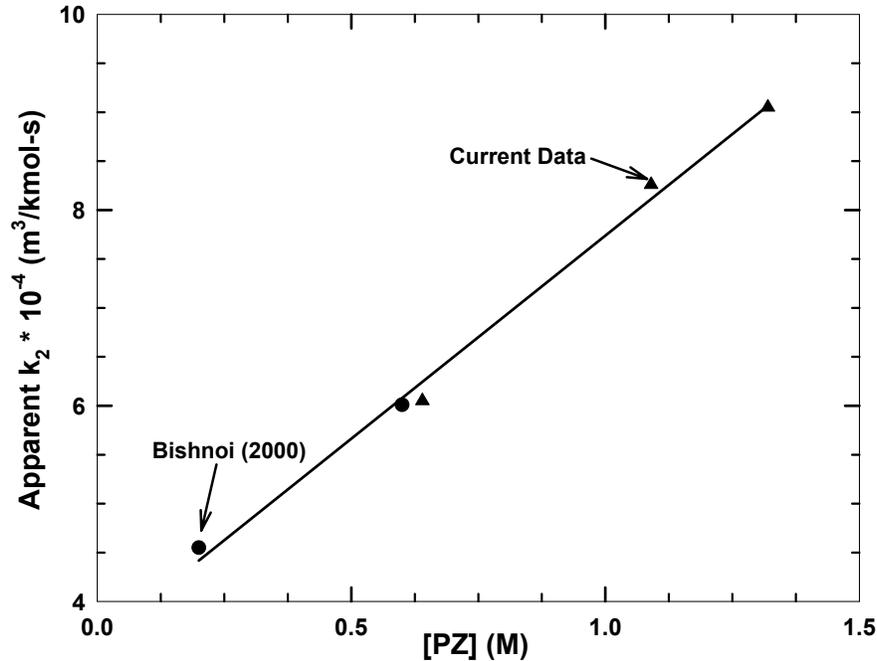
Figure 8. CO$_2$ Absorption Rate of Aqueous PZ at 25°C as Measured in the Wetted-Wall Column

In previous work (Cullinane, 2002), a simple representation of equilibrium was used with the rate model of Bishnoi (2000) where it is apparent that a term accounting for additional enhancement is required at low loadings. An increase in the rate constant of PZ is also observed with the addition of K_2CO_3 suggesting that CO_3^{2-} may contribute to the overall rate in mixed solvents.

Ionic strength has a considerable effect on the rate of CO_2 absorption into aqueous PZ (Figure 9). At 25°C, the apparent rate constant increases by an order of magnitude at 3 M ionic strength. At 60°C, a factor of two increase is observed at 2 M ionic strength. Furthermore, the magnitude of the increase does not appear to be ion specific. Similar results have been obtained in DGA and morpholine by Al-Juaied (2004). This behavior has significant implications for existing processes. Degradation of amines such as MEA produces heat-stable salts; these salts, while a byproduct of amine consumption, may serve to increase the effective rate constant in the degraded solvent and, to a point, actually improve rate performance.
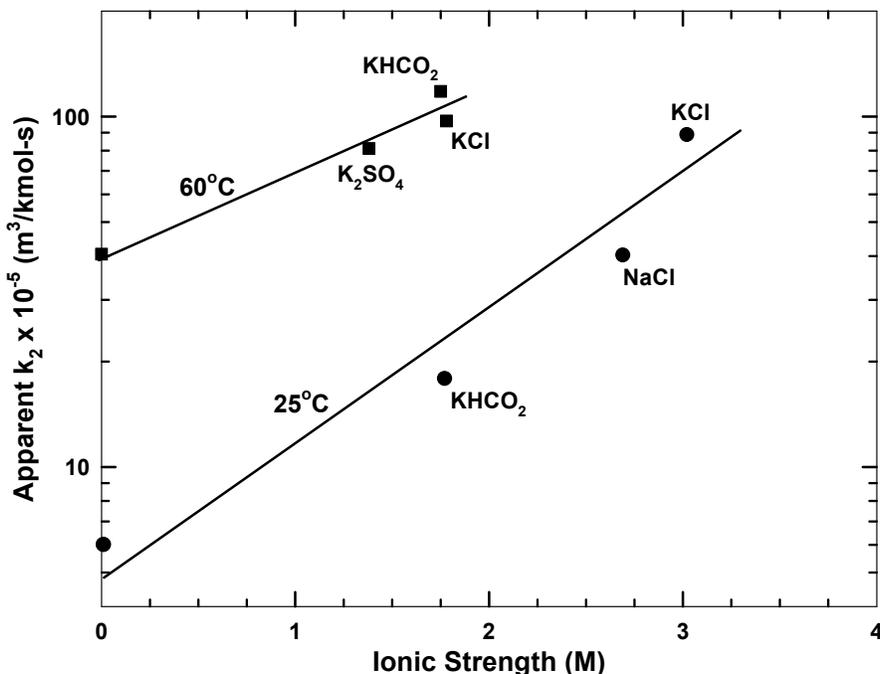
Figure 9. Effect of Ionic Strength on the Apparent Rate Constant of 0.6 M PZ at Loading < 0.05

Conclusions

- The absorption rate of concentrated K^+/PZ mixtures is 1.5 to 5 times faster than the base-case technology, 30 wt% MEA.

- An optimum concentration ratio of 2:1 for K^+ to PZ has been observed in rate experiments. This optimum was confirmed by using the previously developed equilibrium model to predict speciation as a function of this ratio. The optimum is a

result of the tradeoff between buffering the system and reducing protonation, and sacrificing PZ to the carbamate forms by introduction of large quantities of K_2CO_3.

- The temperature behavior demonstrated by k_g' indicates that kinetics control the absorption process at absorber conditions. At stripper conditions, the temperature dependence is small and the process is likely controlled by the diffusion of reactants and products to and from the gas-liquid interface.

- Preliminary modeling of the CO_2 absorption rate in aqueous PZ indicates the mechanism appears to be second order with respect to the amine. Following the "zwitterion" mechanism, other bases, such as hydroxide and carbonate, can be expected to contribute. Values for these rate constants must be regressed from additional data.

- Ionic strength has a significant impact on the rate constants. Rigorous modeling of these ionic strength experiments will be necessary to account for contributions in the K_2CO_3 experiments.

Subtask 1.4a – Predict Stripper Pilot Results – Simple Spreadsheet Model for Stripper

by Babatunde Oyenekan
(Supported by this contract)

Introduction

We have continued to develop the stripper submodel using a simple spreadsheet for an overall model of CO_2 absorption/stripping by an aqueous solution of potassium carbonate and piperazine. This model uses equilibrium stages with Murphree efficiencies. It represents VLE and enthalpies with simple approximations that can be adjusted for a wide variety of solvents and operating conditions. For most practical conditions, the solvent is overstripped to a lean loading that minimizes stripping steam requirement. The effect of stripper pressure (80 – 300kPa), rich and lean $[CO_2]_T$, approach temperature (5-10°C) and the equivalent work consumed by the process are calculated by this model. The results show that the 5 m K+ / 2.5 m PZ can reduce energy consumption by 25 – 46% when compared with 7 m (30 wt%) MEA. Additional heat savings of up to 6% can be achieved by operating the stripper at greater pressure.

Experimental (Model Formulation)

Simple Spreadsheet Model

A simple model has been developed in Microsoft Excel to model the stripper operation. The model was designed for a wide variety of solvents but has currently been applied to a 7 m MEA and a 5 m K^+ / 2.5 m PZ solution.

Modeling Assumptions

(a) The heat of desorption of CO_2 from 7 m MEA ,5 m K^+ / 2.5 m PZ and heat of vaporisation of water are constant at 17.1, 14.3 and 10 kcal/gmol, respectively.

(b) Murphree efficiencies of 40% for CO_2, 100% for water and 100% for heat transfer.

(c) The reboiler was assumed to be in equilibrium.

The CO_2 vapor pressure (kPa) under stripper conditions are represented by the linear expression

$$\ln P = a + b * [CO_2]_T - \frac{c}{T} \tag{23}$$

P = the equilibrium partial pressure of CO_2 in kPa

T = temperature in Kelvin

$[CO_2]_T$ = total CO_2 concentration (m)

The adjustable constants (Table 3) were obtained by regressing the points from the rigorous model for 5 m K+ / 2.5 m PZ by Cullinane et al. (2004) and for MEA equilibrium flashes in AspenPlus™ using the rigorous model developed by Freguia from data of Jou and Mather.

Table 3. CO_2 Vapor Pressure (kPa) at Stripper Conditions as a Function of $[CO_2]_T(m)$ and $T(K)$

	7 m MEA	5 m K+ / 2.5 m PZ
a	20.58	12.80
b	2.04	2.57
c	8612	7788

The partial pressure of water is calculated from the Clausius Clapeyron equation.

$$P_{H2O} = \exp\left(\ln 100 + \frac{10000}{1.987}\left(\frac{1}{T} - \frac{1}{373} \right) \right) \tag{24}$$

From the linear model, the heat of desorption of CO_2 is a function of $[CO_2]_T$ and temperature. For the energy balances in the stripper the average of the heat of desorption between 100 and 120°C was used for the energy balances in the stripper. The heat of desorption of CO_2 from 7 m MEA and 5m K^+ / 2.5 m PZ was 17.1 and 14.3kcal/gmol, respectively. The heat capacity of the solvent was approximated as 1 kcal/kg H_2O-°C while the heat capacity of the gas was neglected.

The model consists of seven stages with a 40% Murphree efficiency on each stage and an equilibrium reboiler. Rich $[CO_2]_T$ corresponding to a partial pressure of CO_2 leaving the absorber at 1.25, 2.5, 5, 10 kPa for different lean $[CO_2]_T$. The CO_2 concentrations on each of the intermediate stages were guessed and the partial pressure of water on each stage was calculated by Equation (24) while Equation (25) was used to calculate the equilibrium partial pressure of CO_2 on each stage.

$$E_{mv} = \frac{P_n - P_{n-1}}{P_n^* - P_{n-1}} \tag{25}$$

where

E_{mv} is the Murphree plate efficiency defined in terms of partial pressures of CO_2

P_n, P_{n-1} are the partial pressures of CO_2 on stages n and n-1

P_n^* is the equilibrium partial pressure of CO_2 leaving stage n.

A composition profile of CO_2 was guessed. Two macros were created and run to (1) set the total pressure of each stage to the desired pressure (which ranged from 80 to 300 kPa), and (2) to set the rich loading to the desired rich loading for the run. The approach temperature was varied between 5 and 10°C

The reboiler duty per gmol CO_2 was calculated as the sum of the heat of desorption of CO_2, the heat of vaporisation of water and the sensible heat required to bring the rich solution to the temperature of the stripper.

$$Q(kcal/gmol) = n_{CO2}\Delta H_{des} + n_{H2O}\Delta H_{vap} + LC_p(T_{lean}-T_{rich}) \qquad (26)$$

The equivalent work is a convenient way to quantify the heat requirement of the process. It constitutes the work lost from the turbine upstream of the power plant since the condensing steam used to run the reboiler is no longer available to generate electric power. Assuming the enthalpy difference between the feed and products is negligible compared to the heat input and cooling water at 313 K is used to remove heat in the condenser, the equivalent work, W_{eq}, consumed by the process is given by

$$W(kcal/gmol\,CO_2) = Q\left[\frac{T_{cond} - T_o}{T_{cond}}\right] + W_{comp} \qquad (27)$$

where Q is the reboiler duty in kcal/gmol CO_2, T_{cond} is the temperature of the condensing steam (temperature of reboiler plus 10K) in the shell of the reboiler and T_o is the temperature of the cooling water (313K). W_{comp} constitutes the adiabatic work of compression of the gas exiting the top of the stripper to 300 kPa (an arbitrary pressure selected). For this analysis isentropic efficiency of the compressor was assumed to be 75%.

Results and Discussion

Predicted Stripper Performance

The above described model was used to calculate the reboiler heat duty required for a given rich and lean $[CO_2]_T$. For most runs, the pressure was set as 160 kPa and the rich solution was preheated to 10^oC cooler than the lean solution leaving the stripper. The lean solution was adjusted to minimize the steam requirement (kcal/gmol CO_2) for a specified rich loading corresponding to equilibrium CO_2 pressures of 1.25, 2.5, 5, 10 kPa when the absorber operates at 40 and 60^oC, respectively.

Figure 10 shows the minimum reboiler duty and optimum capacity as a function of $[CO_2]_T$ for the two solvents with a 10^oC approach. The reboiler duty decreases by a factor of two over the practical range of rich $[CO_2]_T$. The optimum capacity of 5 m K^+ / 2.5 m PZ is 0.22m greater than that of 7 m MEA. Since 5 m K^+ / 2.5 m PZ has a faster rate, the absorber can be operated at a closer approach to saturation and a greater partial pressure than 7 m MEA.

Figure 11 shows the minimum reboiler heat duty (kcal/kg H_2O) and optimum lean CO_2 concentration for 5 m K^+/2.5 m PZ and 7 m MEA at 160 kPa with a 10^oC approach. It is observed that the reboiler duty decreases with increasing $[CO_2]_T$ concentration. At a fixed partial pressure, the optimum heat duty required for 7 m MEA is 5 kcal/kg H_2O greater than that for 5 m K^+/ 2.5 m PZ. This means less of the 5 m K^+/ 2.5 m PZ solvent will be required to strip CO_2 which results in a lower solvent cost. The optimum lean $[CO_2]_T$ concentration is relatively constant for both solvents. This implies that the optimum heat requirement is independent of the lean loading and depends only on the rich $[CO_2]_T$ concentration.
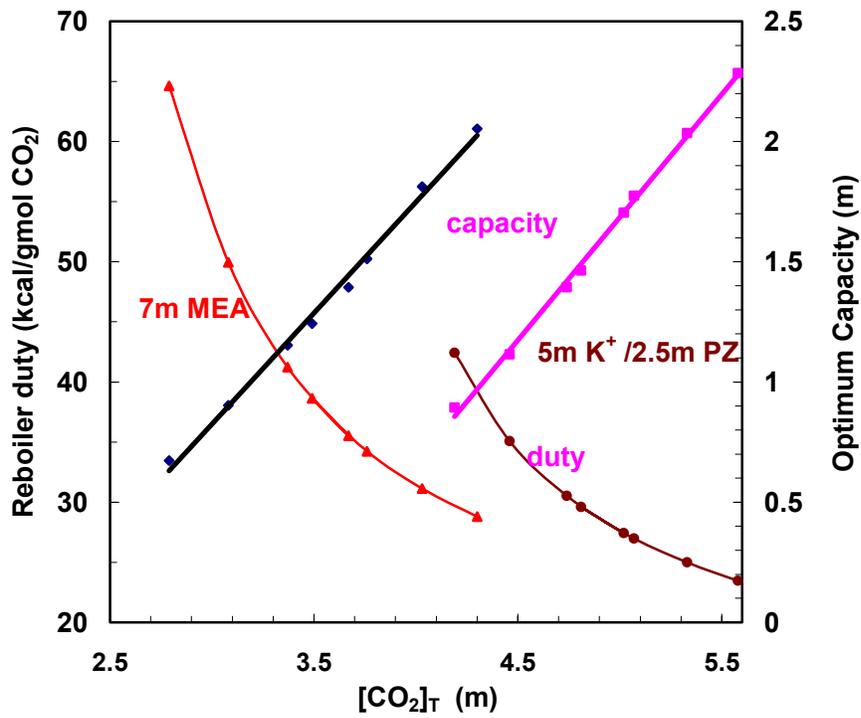
Figure 10. Optimum Stripper Performance, 160 Kpa, 10°C Approach
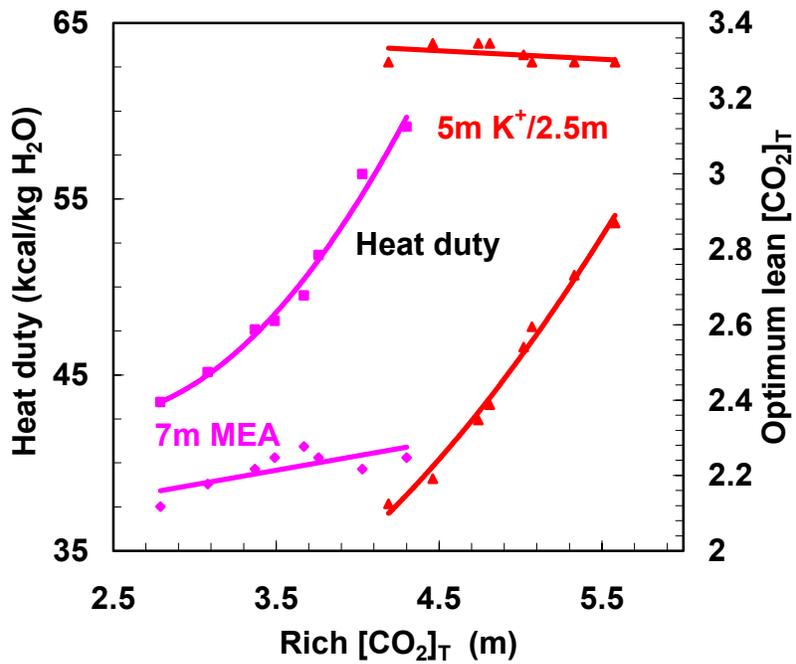
Figure 11. Optimum Heat Duty and Lean [CO$_2$]$_T$ for Solvents, 10°CApproach

The reboiler duty as a function of the CO_2 vapor pressure of the rich solution at 40^oC and 60^oC is shown in Figure 12. As with the rich loading, the reboiler duty decreases a factor of two over the range of rich CO_2 vapor pressure. At a given rich vapor pressure, 7 m MEA requires 18-34% more heat than 5 m K^+/2.5 m PZ. However, because of the difference in mass transfer rates, 7 m MEA must operate at a rich CO_2 vapor pressure of 5 kPa when 5 m K^+/2.5 m PZ can be run at 10 kPa. At these conditions, when the absorber is run at 60^oC, 5 m K^+/2.5 m PZ will require 35% less heat than 7 m MEA. If the vapor pressure achieved by 5 m K+/2.5 m PZ is always twice that of 7 m MEA, the range of energy savings is 25 – 46%.
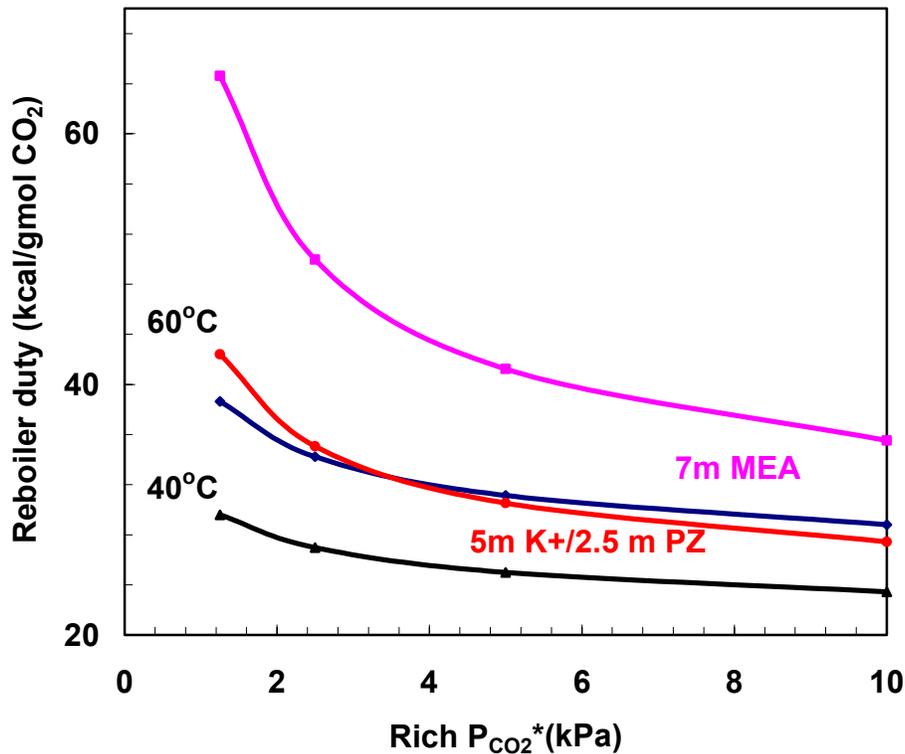
Figure 12. Optimum Reboiler Duty, 160 kPa, 10^oC Approach

Figure 13 shows the reboiler duty and optimum capacity for 5 m K^+/2.5 m PZ. The reboiler duty is reduced 0 to 6% by increasing the stripper pressure from 160 to 300 kPa. The effect is less pronounced with richer feed. It is usually infeasible to operate the stripper above 120^oC when MEA solutions are used as MEA is subject to degradation by polymerization at higher temperatures. Piperazine is not an alkanolamine and is not subject to the same mechanisms of degradation as MEA and so it should be possible to operate the stripper at greater pressure with the 5 m K^+/2.5 m PZ solution.
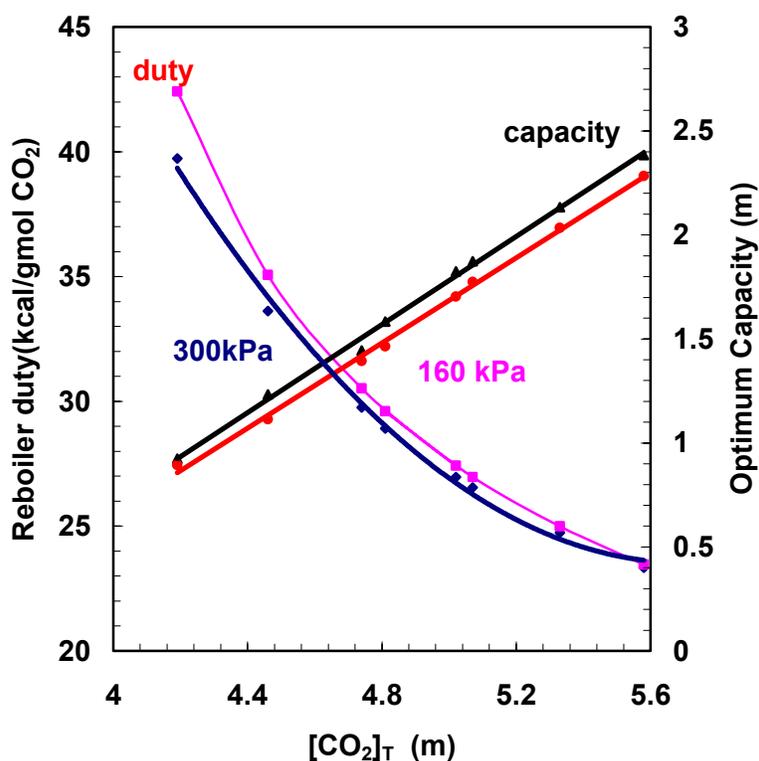
Figure 13. Stripper Performance at Elevated Pressure, 5 m K$^+$/2.5 mPZ, 10°C Approach

Over the range of achievable rich solution compositions, the equivalent work for 7 m MEA varies from 6 to 14 kcal/gmol CO_2 (Figure 14). The equivalent work for 5 m K$^+$/2.5 m PZ (4.2 to 9 kcal/gmol CO_2) is about 29% lower. This means that the energy saved by using the 5 m K$^+$/2.5 m PZ can be expanded in the turbines upstream of the power plant generating more work that could be used in the production of electricity.

Figure 15 shows that when 5 m K$^+$/2.5 m PZ is used as the solvent the equivalent work increases by 0.6 kcal/gmol CO_2 over the entire range of CO_2 concentrations when the stripper pressure is increased from 80 kPa to 300 kPa. . The reboiler temperatures are about 90°C and 130°C, respectively. MEA degrades at high temperatures due to poly-merization and as such are not feasible for operations above 120°C.
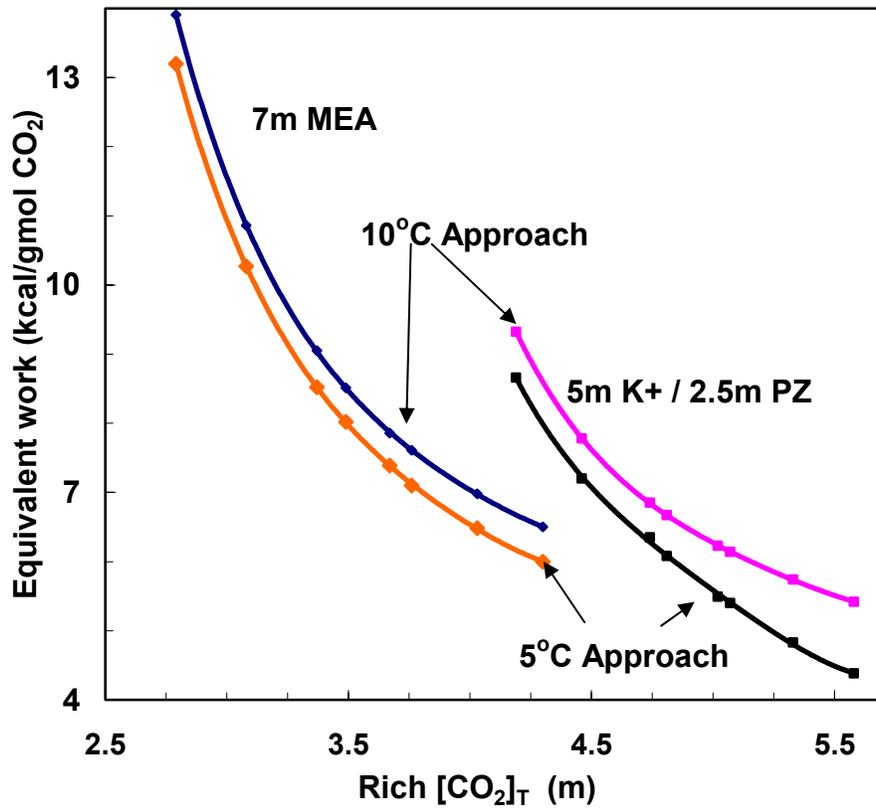
Figure 14. Equivalent Work Consumed by the Stripper for 7 m MEA and 5 m K+/ 2.5 m PZ, P_T = 160 kPa
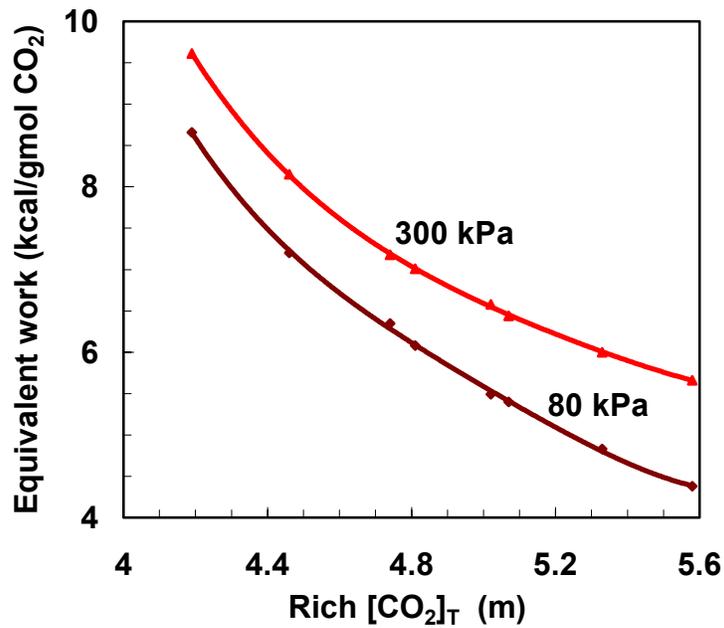
Figure 15. Work Consumed by the Stripper for 5 m K+/ 2.5 m PZ, $\Delta T = 10^oC$

The McCabe-Thiele diagram for the stripper when the reboiler heat duty is minimized for 5 m K+/ 2.5 m PZ with a rich $[CO_2]_T$ of 4.46m is shown in Figure 16. It shows that at this concentration flashing of the solution takes place at the top of the stripper. A rich pinch is also experienced at the top of the stripper in the first two stages. A substantial part of the stripping operation takes place in stages 3 through 7. The lean $[CO_2]_T$ that minimizes heat requirement is 3.35 m. This is less than that required for 90% CO_2 removal with a 30% approach to equilibrium in the absorber ($[CO_2]_T$ = 3.85 m). If the solution is stripped further as in Figure 17, a lean end pinch is observed. This requires more reboiler heat duty which suggests that over stripping of the solution is an attractive option to minimize the heat requirement.
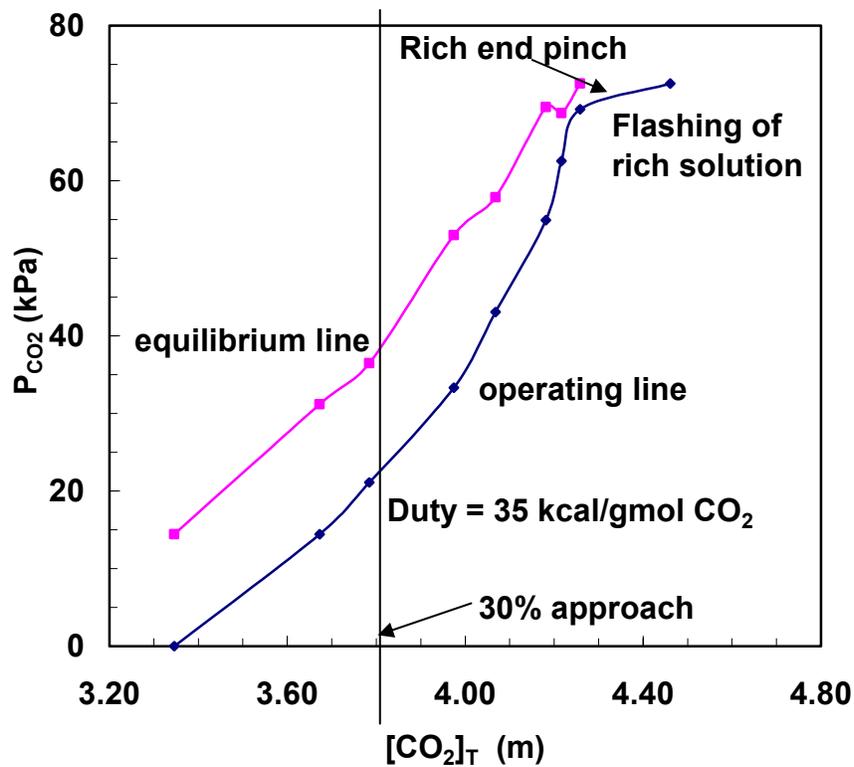
Figure 16. McCabe-Thiele Plot for 5 m K+/ 2.5 m PZ at Rich $[CO_2]_T$ = 4.46m, Lean $[CO_2]_T$ = 3.35 m, PT= 160 kPa, $\Delta T = 10^oC$, Optimum Solvent Composition
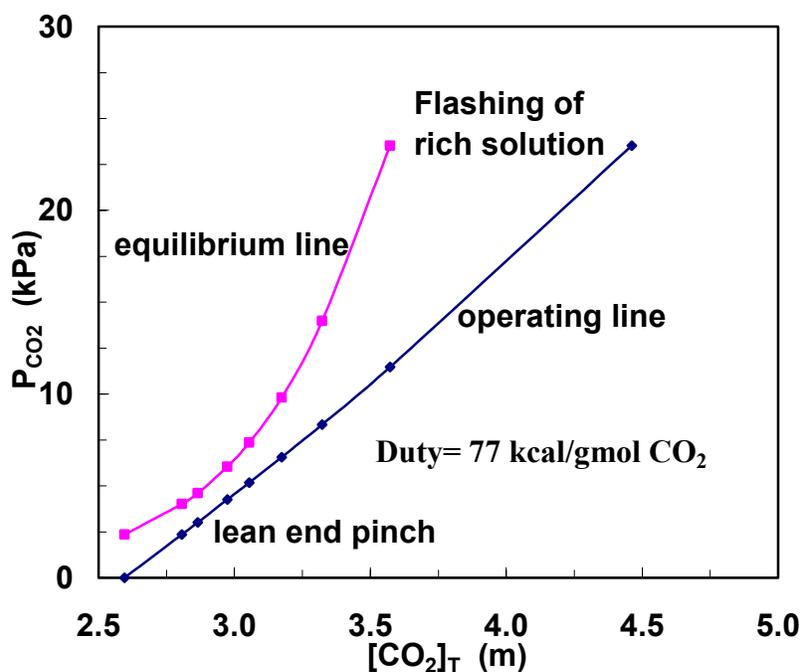
Figure 17. McCabe-Thiele Plot for 5 m K+/ 2.5 m PZ at Rich $[CO_2]_T$ = 4.46m, Lean $[CO_2]_T$ = 2.6m, P_T = 160 kPa, ΔT = 10°C, Lower Than Solvent Composition

Conclusions and Future Work

In this quarter, the simple spreadsheet model to predict pilot plant performance was modified and applied to 7 m MEA and 5 m K$^+$ / 2.5 m PZ. The results show that 7 m MEA requires 18-34% more heat than 5 m K+/ 2.5 m PZ when a 10°C approach is used and the stripper operated at 160 kPa. If the CO_2 vapor pressure is always twice that of 7 m MEA, the energy savings range from 25- 46%. Additional savings up to 6% can be achieved by operating the stripper at 300 kPa. The work consumption of the process varies slightly from 80 – 300 kPa using the 5 m K+/ 2.5 m PZ solution so the stripper can be operated at any convenient pressure. For most practical situations, the solvent is over-stripped in order to minimize energy requirement. In the next quarter, this work will be extended to an innovative stripper configuration to reduce steam requirements.

Subtask 1.4b – Predict Absorber Pilot Results

by Jennifer Lu
(Supported by various industrial donors)

Introduction

This report presents the continuing development of an absorber model in Aspen Plus™ for use in modeling the pilot plant. The model is based on the existing 30% MEA-system model by Freguia (2002) and altered in order to make the MEA system emulate a system that uses potassium carbonate promoted by piperazine. Results from comparing the 30% MEA-system model and the modified PZ model were obtained. Refinements to the model to include structured packing and K^+ are underway.

Experimental

Simulations using a 30% MEA solvent and the PZ solvent were performed at the conditions in Table 4.

Table 4. Simulation Conditions

Removal (%)	Solvent	Packing (m)	$P^*_{CO2,lean}$ (Pa)
90	K^+/PZ	15	39.3
90	MEA	15	40.1
75	K^+/PZ	6.1	39.3
90	K^+/PZ	6.1	39.3
75	MEA	6.1	40.1

The packing type is CMR #2 and the lean partial pressure is calculated at 60°C.

The simulation was also modified to include structured packing. A new FORTRAN subroutine was added to the simulation. The subroutine inputs a value from the user and sets the interfacial area equal to the value. The kinetic subroutine was also modified to reflect the interfacial area. The user must input the interfacial area, taken from Wilson (2004), and enter the value in two places.

Additionally, the potassium ion was added to the component list in the 30% MEA-system simulation. The kinetic subroutine was reconfigured to facilitate adding components. Compositions are now in the form "x(IMEA)" instead of "x(3)".

Results and Discussion

The MEA and PZ results are shown in Table 5 below. The vapor pressure of the rich solution, $P^*_{CO2,rich}$, was calculated at 60^oC.

Table 5. Simulation Results

Removal (%)	Solvent	Packing (m)	Capacity (m)	Rich Ldg (m)	$P^*_{CO2,rich}$ (Pa)
90	PZ	15	2.22	6.16	6741
90	MEA	15	2.14	3.38	5846
75	PZ	6.1	2.13	6.07	5062
90	PZ	6.1	1.87	5.80	2221
75	MEA	6.1	1.76	3.00	1701

In all cases, for the same amount of packing, the PZ solvent gives a richer solution and a higher rich partial pressure. With 15 m of packing, the PZ solvent has a higher rich loading and a higher rich partial pressure. With 6.1 m (20 ft) of packing, the PZ solvent achieves the same removal as the MEA solvent, with a much higher rich partial pressure, nearly 4 times greater. The PZ solvent can also achieve better removal with greater capacity and higher rich partial pressure, although the partial pressure increase is not as great.

Clearly, the PZ solvent performs better than the MEA solvent. However, the increase in performance is more pronounced when more packing is used. It is not understood why this is.

The structured packing subroutine was added to the simulation, but all attempts to run the simulation met with failure. Not only does the simulation not run, Aspen completely crashes and must be restarted. The interfacial area change to the kinetic subroutine was successful.

The potassium ion was added to the simulation. Altering the kinetic subroutine was successful, although running the simulation with the added ion was not. The number of iterations was increased in an attempt to help the simulation converge. A working simulation was produced, but the file was corrupted. Work is underway to reconverge a new file.

Future Work

As the refinements to the simulation are implemented, pilot plant performance will be modeled. Once the interaction parameters for MEA and K^+ and PZ and K^+ are available, they will be added to the simulation.

Task 2 – Pilot Plant Testing

Subtask 2.1d – Piperazine and Potassium Analysis by Acid-Base Titration

by Ross Dugas
(Supported as a Teaching Assistant and by this contract)

Introduction

In the pilot plant, it is necessary to determine the composition of the amine solution. A titration is being used to determine the piperazine and the potassium concentrations of the solution.

Experimental

Titrating with HCl will give a total alkalinity in the sample. Since piperazine has two equivalents per mole and potassium only has one, the total alkalinity will be the potassium concentration plus double the piperazine concentration. The endpoint of the titration can be seen using methyl orange indicator which will turn bright orange when the all the piperazine and potassium have reacted.

From this point, titrating back up the pH range with NaOH will yield the piperazine concentration since only the PZ will react with the NaOH, again on a two equivalents per mole basis. From here one can easily determine the potassium concentration. Unfortunately the remaining carbon dioxide in solution after the HCl titration can skew the results of the second titration so it is necessary to remove the excess carbon dioxide between titrations. Currently, boiling the solution while stirring is the preferred method of removal. In order to determine the endpoint of this second titration with NaOH, a pH meter was required.

A known solution was formulated and the predicted amounts of HCl and NaOH were calculated. The volume of HCl needed to reach the endpoint proved virtually identical to the calculations. After the solution was boiled and cooled to ambient temperature, the calculated amount of NaOH was added and the millivolt response of the pH electrode was observed. For the calculated amount of NaOH added, the pH meter yielded a reading of $\approx$ -265 mV. The solution must be at ambient temperature since the mV reading is affected by temperature. This value of -265 mV was used as the endpoint of the NaOH titration.

A standard operating procedure was prepared. The standard operating procedure (SOP) can be seen at the end of this section of the report.

The experimental procedure yields results in a kilogram sample basis. In order to get results in a molality terms, the components were assumed to be in the forms of piperazine, potassium carbonate, and carbon dioxide. This is the most straight forward basis since this is how the solutions are formulated in the industrial environment, as opposed to laboratory environment which may use potassium bicarbonate instead of

gaseous CO_2. A total organic carbon analyzer was used to determine the CO_2 concentration.

Results and Discussion

Four compositions were used in the first campaign of the pilot plant. The composition results of runs near the beginning and end of each solution composition can be seen below in Table 6.

Table 6. Piperazine and Potassium Concentrations for Pilot Plant Runs

Sample		PZ Conc. (molality)	K^+ Conc. (molality)
Date	Time		
6/16/2004	15:30	1.75	2.93
6/16/2004	17:00	1.69	2.94
Composition Change			
6/17/2004	11:30	1.67	3.29
6/21/2004	16:30	1.66	3.36
Composition Change			
6/22/2004	18:30	2.23	4.57
6/24/2004	12:30	2.41	4.94
Composition Change			
6/24/2004	15:45	2.64	5.21
6/24/2004	17:00	2.63	5.39

At the last two compositions, both final solutions are more concentrated than the earlier solutions. This may be due to loss of water throughout the process or possibly a higher water accumulator level in the system. Some intermediate runs will be tested to determine if this is a gradual change which would indicate steady water loss or a more sudden change indicating a new liquid level in the accumulator.

Procedure for Piperazine and Potassium by Titration

1. Tare a 100 mL beaker on a scale.

2. Using a pipette, add 10 mL of sample to the beaker and record the mass.

3. Add approximately 5 drops of methyl orange indicator to the sample.

4. Using a magnetic stir bar, stir the sample on a hot plate stirrer.

5. Fill one buret with certified 2N (±0.005) HCl.

6. Record the starting volume of HCl in the HCl buret.

7. Slowly add HCl to the solution until the sample turns from yellow to orange.

8. Record the final volume of HCl in the HCl buret.

9. On the hot plate stirrer, heat the sample to a boil to release CO_2 out of the solution.

10. Rapidly boil the solution for 2 minutes while still stirring it with the magnetic stir bar.

11. After 2 minutes, turn off the heat and allow the solution to return to ambient temperature.

12. Fill a second buret with certified 2N (± 0.02) NaOH.

13. Record the starting volume of NaOH in the NaOH buret.

14. Magnetically stir the solution while immersing a pH meter in the sample.

15. Add NaOH to the solution until the pH meter gives a reading of ≈ -265 mV.

16. Record the final volume of NaOH in the NaOH buret.

Subtask 2.3 – Install and Modify Equipment

by Eric Chen
(Supported by EPA Star Fellowship)

In this quarter, all of the pilot plant modifications were completed. Two 8-inch PVC lines were installed. One line connects the existing PVC airline to the inlet of the absorber column and other line connects the blower inlet to the stainless steel pipe from the absorber outlet. A 2-inch line was installed to connect the CO_2 return from the stripper downstream of the blower. Installation of the process instrumentation and the Delta V graphical user interface (GUI) was completed. Vaisala CO_2 gas analyzers were installed at the inlet and the outlet of the absorber. A COA storage rack was constructed and ½-inch stainless steel tubing was run for CO_2 makeup. In addition, a CO_2 gas sample/calibration panel was fabricated. Quarter-inch polyethylene tubing was run from the sample panel to the inlet, middle, and outlet of the absorber column and CO_2 analyzer calibration chambers. The annubar and pressure transmitter and pH probes were installed.

Subtask 2.4 – Campaign 1 – Base Case

by Eric Chen
(Supported by EPA Star Fellowship)

Summary

Campaign 1 of the CO_2 capture pilot plant was completed in late June. Nineteen runs were conducted with three solvent compositions containing potassium and piperazine concentrations at 2.3, 2.9, and 3.1 mol K^+/kg solvent and at 1.15, 1.45, and 1.55 mol PZ/kg solvent, respectively. The gas and liquid flowrates varied from 0.5 to 3 kg/m^2-s and 1.3 to 5.1 kg/m^2-s, respectively. The L/G ratio varied from 0.9 to 5.6 kg/kg. The synthetic flue gas contained 3 and 12 % CO_2 in air. The stripper pressure varied from 1 to 1.7 atm. The absorber contained 20 ft of Flexipac™ 1Y structured packing and the stripper contained 13 sieve trays with 18-inch tray spacing. Lean loading and CO_2 penetration varied from 0.41 to 0.54 mol CO_2/total alkalinity and 0.2 to 15.8%, respectively. Vanadium was used at 18 mmol/kg solution (1000 ppm) to inhibit corrosion. Dissolved iron concentration varied from 0.3 to 0.6 mmol/kg solution.

Experimental – Pilot Plant Operations

Pilot plant operations commenced at the end of May. First, the effective area of the absorber was determined by absorbing CO_2 from ambient air into a solution of 0.1 N potassium hydroxide (KOH). The gas and liquid flowrates varied from 180 to 450 acfm and 5 to 25 gpm/ft^2, respectively. The starting solution inventory was approximately 800 gallons (14 drums). A Horiba VIA510 was used to measure the outlet CO_2 concentration, which has a range up to 500 ppm.

Upon completion of the effective area tests, five drums of the 0.1 N KOH solution were removed. The remaining solution was mixed with 3 drums of 68% piperazine AQ, 2 drums of water, 5 drums of 47% liquid K_2CO_3, and 7.75 gallons of the HotPot solution. Piperazine has a freezing point of 130°F and is solid at room temperature. Drum heaters were used to facilitate the chemical loading process. Numerous attempts to solubilize piperazine in the potassium carbonate solution were unsuccessful. The piperazine was eventually loaded by pumping hot bicarbonate solution into the drum and back into the system. While the solvent was circulating, 50 mL of anti-foam was added to the system to correct the foaming issue.

Once the chemicals were loaded, troubleshooting on the absorber and stripper began. It was discovered early on that the some of the piperazine had precipitated at the bottom of the absorber tank. Hot solvent was circulated through the entire system to dissolve the piperazine and feed was drawn from the side of the absorber feed tank, instead of the bottom. The pilot plant was operated for a total of 7 days, beginning in mid-June.

The online absorber inlet and outlet CO_2 concentrations were measured with Vaisala GM CO_2 analyzers. The Vaisala probes were ranged from 0-1%, 0-5% and 0-20% CO_2. The online absorber middle concentration was measured using a Horiba PIR-

2000 CO_2 analyzer, which had a range of 0-5 % CO_2. The Horiba analyzer could be readily switched to sample the inlet, outlet, or middle of the absorber. The Vaisala measurements were confirmed by the Horiba. The CO_2 analyzers were calibrated before the start of the campaign, on the 18th, 23rd, and 24th. At higher CO_2 concentrations, the Horiba analyzer was over-ranged and could not read certain absorber middle concentrations.

Liquid samples were taken at the inlet, middle, and outlet of the absorber. The pH and temperatures were recorded for each off line sample with a handheld pH meter. The majority of the samples from the various runs have been analyzed. Piperazine and potassium concentrations were determined by titration with hydrochloric acid and sodium hydroxide and the total was reported as total alkalinity. CO_2 loading was determined by a total organic carbon analyzer (TOC) operating in the mode that gives inorganic carbon. Piperazine and potassium concentration was verified by TOC and inductively coupled plasma (ICP) analysis, respectively. Vanadium and total iron were determined by ICP.

The CO_2 makeup system was modified by the addition of two hairpin heat-exchangers. The steam heated regulator that was originally purchased was undersized. Even at low flowrates, the CO_2 makeup line would freeze. The heat exchangers were constructed using ½ and ¾ stainless tubing and Swagelok fittings. The CO_2 makeup system was under-designed for the large flowrates that were necessary to inventory the system, but it was more than adequate for CO_2 makeup.

Based on the amount of CO_2 makeup, there was little leakage from the system. Any CO_2 losses may have come through the space between in the blower hub and casing and from two ¾-inch penetrations downstream of the knockout pot. When the two penetrations were sealed, the absorber operated under vacuum, which appeared to affect the Vaisala CO_2 measurement by causing air to leak in through the fitting and dilute the measurement. Opening the two holes appeared to reduce the vacuum and eliminate any leaks through the Vaisala fittings.

Based on empirical observations, the gas came to steady state within 5-10 minutes after a change in condition. However, based on the data, it appears that the liquid inside the absorber sump may not have reached steady state as quickly as the gas. The liquid inside the absorber packing is plug flow, while the sump acts as continuous stirred reactor (CSTR) and reaches steady state later. Therefore, the sump composition will be different from the liquid in the column since it reaches steady state at a later time. The rich liquid samples were withdrawn downstream of the absorber sump.

The absorber inlet temperature and stripper outlet temperatures were well controlled. The liquid inlet temperature was maintained at approximately 313 K through the campaign, with the exception of the last four runs. The inlet liquid temperature was maintained at about 319 K because the solution was more concentrated. The inlet gas temperature varied from 300 to 320 K and was systematically low because the gas cooler could not be turned off completely.

The solvent preheater did not function as designed because the steam traps were improperly sized. Condensate built up in the traps and backed up in the heat exchanger. Therefore, rich solvent feed was in the temperature range of 343 to 361 K. As a result, stripper steam duties were high and the regeneration capacity was low. This limited the

upper range of gas rates that could be run in the absorber. The stripper pressure varied from 1 to 1.7 atm. In the future, the stripper will be operated at higher pressures to help facilitate CO_2 steam stripping requirements.

The pressure drop in the absorber ranged from 0.05 to 0.66 inches of H_2O/ft packing. The pressure drop in the top bed was typically slightly higher than the bottom bed. This is due to the temperature bulge in the top bed. The higher gas temperature decreases the density of the gas and results in a higher pressure drop. The column was not operated near the flooding point.

About 375 ml of anti-foam was added to the solvent system over the course of pilot plant operations. The online Rosemount pH meters failed after the first day of the operation. The rain may have short-circuited the probes because the pH meter connections were not design for outdoor use. Both the absorber and stripper filters eventually plugged up and were operated on bypass. It appeared that the stripper had plugged up with potassium carbonate and the absorber filter with piperazine. The pressure transmitters for the reboiler and stripper sump levels also plugged up during the course of operations. The instrument lines were unplugged and operations resumed.

Results and Discussion

The results from the KOH test show that the maximum effective area is approximately 49% of the total packing surface area. The dry specific area of the Flexipac™ 1Y structured packing is 410 m^2/m^3. The results are plotted in Figure 18. The figure shows that at higher gas rates, the effective area appears to approach a maximum. These results are consistent with those obtained by UT-SRP (Separations Research Program) for another high-surface-area structured packing.

The results from the absorption of CO_2 into the piperazine/potassium carbonate solvent are shown in Tables 7 and 8. Table 7 shows the absorber analyses results. Table 8 shows the absorber operating conditions and the results for the various runs. Nineteen runs were conducted with three solvent compositions containing potassium and piperazine concentrations at 2.3, 2.9, and 3.1 mol K^+/kg solution and at 1.15, 1.45, and 1.55 mol PZ/kg solution, respectively. The gas and liquid flowrates varied from 0.5 to 3 kg/m^2-s and 1.3 to 5.1 kg/m^2-s, respectively. The L/G ratio varied from 0.9 to 5.6 kg/kg. The synthetic flue gas contained 3 and 12 % CO_2 in air. The absorber pressure was operated at 1 atm. The stripper pressure varied from 1 to 1.7 atm. Lean loading and CO_2 penetration varied from 0.41 to 0.54 mol CO_2/total alkalinity and 0.2 to 15.8%, respectively. Vanadium concentrations were maintained at approximately 18 mmol/kg solution (1000 ppm). Dissolved iron concentration varied from 0.3 to 0.6 mmol/kg solution.
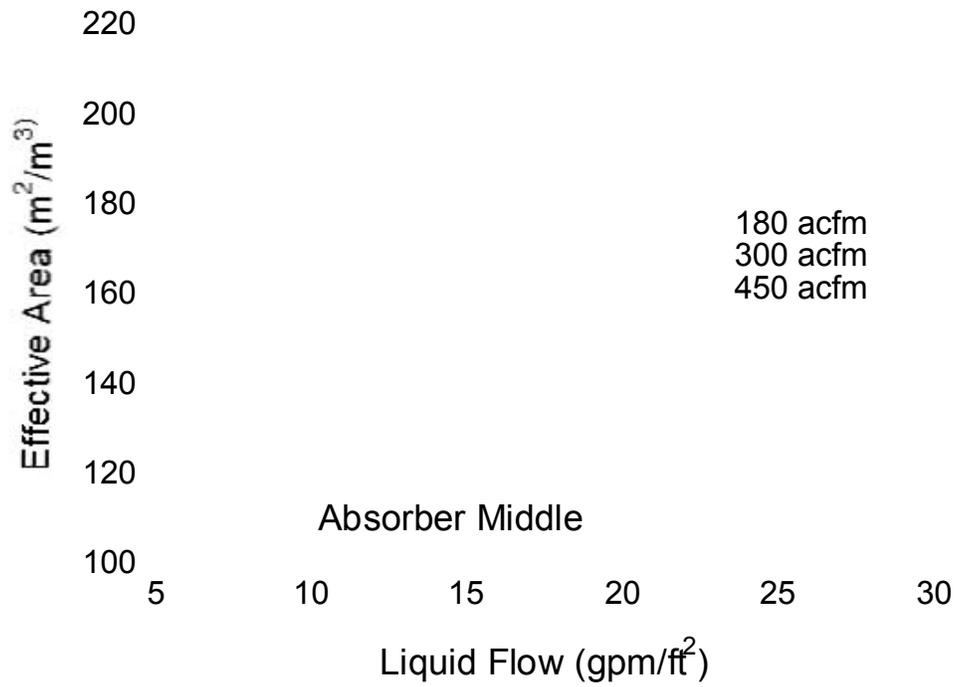
Figure 18. Flexipac™ 1Y Effective Area for CO$_2$ Absorption in 0.1 N KOH

Table 7. Campaign 1 Absorber Analyses Table

Run#	Date	Time	Ln T Alk[1] 2PZ+K+	Titration Lean PZ[2] mol/kg	Titration Lean K+[2] mol/kg	ICP Lean K+[2] mol/kg	ICP Lean V mmol/kg[2]	ICP Lean Fe mmol/kg[2]	TOC[5] Lean PZ mol/kg[2]	TOC[5] Lean CO₂ mol/kg[2]	GC PZ mol/kg[2]	Lean Density[4] kg/m³	Lean Temp[4] K	Lean pH
1.1.1	6/16/2004	15:30	4.51	1.22	2.06	2.00	18.8	0.118	1.09	2.18	-	1145.6	312.7	11.5
1.1.2	6/16/2004	16:15	4.50	1.21	2.08	-	-	0.172	1.17	1.84	-	1145.3	312.3	11.6
1.1.3	6/16/2004	17:00	4.50	1.20	2.10	1.72	18.2	0.172	1.27	1.91	-	1146.6	312.2	11.4
Added 3/4 Drum of K2CO3														
1.2.1	6/17/2004	11:30	4.65	1.17	2.31	2.11	18.0	0.161	1.15	2.03	-	1165.0	313.1	11.5
1.2.2	6/17/2004	12:15	4.59	1.15	2.30	-	-	-	1.09	2.46	-	1162.9	314.9	11.4
1.2.3	6/17/2004	13:00	4.58	1.15	2.29	-	-	-	1.16	2.02	-	1162.4	317.0	11.5
1.3.1	6/17/2004	16:15	4.63	1.16	2.31	-	-	-	1.19	2.19	-	1164.3	314.7	11.2
1.3.2	6/17/2004	16:45	4.64	1.16	2.32	-	-	-	1.22	2.30	-	1165.0	314.1	11.3
1.3.3	6/17/2004	17:45	4.66	1.16	2.33	-	-	-	1.22	2.25	-	1165.5	313.7	11.2
1.4.1	6/17/2004	18:30	4.68	1.17	2.34	-	-	-	1.24	2.31	-	1166.3	313.2	11.3
1.5.1	6/17/2004	19:15	4.67	1.17	2.34	-	-	-	1.29	2.36	-	1166.2	313.3	11.1
1.6.1	6/18/2004	15:30	4.67	1.17	2.33	-	-	-	1.20	2.21	-	1165.9	312.6	10.9
1.7.1	6/21/2004	16:45	4.63	1.15	2.33	1.98	18.1	0.241	1.24	2.25	-	1162.8	313.7	10.6
Removed Water														
1.8.1	6/22/2004	17:45	5.66	1.40	2.87	1.87	18.6	0.172	1.41	2.63	-	1206.1	314.2	10.9
1.8.2	6/22/2004	18:30	5.62	1.39	2.84	-	-	-	1.48	2.66	-	1207.3	314.6	10.9
1.9.1	6/22/2004	19:30	5.59	1.38	2.83	-	-	-	1.46	2.63	-	1206.4	314.6	11.0
1.9.2	6/22/2004	20:15	5.60	1.38	2.83	-	-	-	1.44	2.67	-	1206.7	314.7	11.0
1.10.1	6/22/2004	21:15	5.63	1.39	2.85	-	-	-	1.49	2.76	-	1207.7	314.7	11.2
1.10.2	6/22/2004	22:00	5.63	1.39	2.85	-	-	-	1.44	2.70	-	1207.9	314.7	10.8
1.11.1	6/23/2004	8:15	5.74	1.42	2.91	-	-	-	1.47	2.75	-	1212.6	307.8	9.8
1.11.2	6/23/2004	9:00	5.71	1.41	2.89	-	-	-	1.46	2.84	-	1211.0	308.4	10.6
1.12.1	6/23/2004	14:30	5.71	1.41	2.89	-	-	-	1.44	2.93	-	1211.1	312.9	11.0
1.12.2	6/23/2004	15:15	5.71	1.41	2.89	-	-	-	1.28	3.37	-	1211.2	312.9	11.0
1.13.1	6/23/2004	17:30	5.71	1.41	2.89	-	-	-	1.36	2.94	-	1211.3	313.6	11.1
1.14.1	6/23/2004	18:15	5.73	1.41	2.90	-	-	-	1.41	3.07	-	1211.9	313.5	11.1
1.15.1	6/24/2004	9:00	5.85	1.45	2.96	-	-	-	1.42	3.05	-	1217.0	311.3	10.8
1.15.2	6/24/2004	9:30	5.79	1.43	2.93	-	-	-	1.49	3.08	-	1214.3	315.7	11.0
1.16.1	6/24/2004	10:30	5.73	1.42	2.90	-	-	-	1.48	3.09	-	1212.1	316.8	11.1
1.16.2	6/24/2004	11:00	5.75	1.42	2.91	-	-	-	1.48	3.09	-	1212.7	315.8	11.1
1.17.1	6/24/2004	12:15	5.77	1.43	2.92	-	-	-	1.42	3.12	-	1213.7	314.6	10.9
1.17.2	6/24/2004	12:30	5.84	1.44	2.96	2.42	22.0	0.593	1.48	3.15	-	1213.6	314.4	10.8
Removed Water														
1.18.1	6/24/2004	16:00	6.11	1.54	3.03	2.75	23.6	0.236	1.50	3.25	-	1228.9	319.5	11.0
1.18.2	6/24/2004	16:15	6.19	1.54	3.10	-	-	-	1.39	3.20	-	1228.4	319.3	11.0
1.19.1	6/24/2004	17:00	6.20	1.55	3.11	-	-	-	1.53	3.31	-	1229.0	318.5	11.0
1.19.2	6/24/2004	17:30	6.15	1.52	3.11	2.77	22.9	0.129	1.48	3.24	-	1228.1	318.3	11.2

1. Ln T Alk – Lean total alkalinity defined as $2*PZ+K^+$
2. Defined as mol/kg of solution or mmol/kg of solution
3. Calculated as: Total alkalinity – 2*PZ
4. Measured online
5. TOC measured total carbon (TC) and inorganic carbon (IC). CO_2 determined from IC analysis and piperazine from TC-IC.

Table 8. Campaign 1 Absorber Results Table

Run#	Date	Time	Ln Total Alkalinity 2PZ+K [4]	Lean PZ mol/kg [4]	Loading mol/Alk [1]	K+/PZ [3]	Capacity Liq mol/kg [4]	Capacity Gas mol/kg [4]	CO_2 In %	CO_2 Out %	CO_2 Penetration [2] %	G kg/m2-s	L kg/m2-s	L/G kg/kg	Temp Gas In K	Temp Gas Out K	Temp Liq In K	Temp Liq Out K
1.1.1	6/16/2004	15:30	4.51	1.22	0.48	1.68	0.38	0.88	3.00	0.1612	5.37	2.28	2.53	1.11	306.62	-	312.7	302.3
1.1.2	6/16/2004	16:15	4.50	1.21	0.41	1.71	0.70	0.89	3.00	0.1703	5.67	2.28	2.53	1.11	305.46	-	312.3	302.1
1.1.3	6/16/2004	17:00	4.50	1.20	0.43	1.75	0.68	0.88	3.00	0.1695	5.65	2.27	2.53	1.11	306.60	-	312.2	301.9
Added 3/4 Drum of K2CO3																		
1.2.1	6/17/2004	11:30	4.65	1.17	0.44	1.97	0.37	0.46	2.97	0.0056	0.19	1.14	2.57	2.25	305.35	-	313.1	305.2
1.2.2	6/17/2004	12:15	4.59	1.15	0.54	2.00	0.09	0.46	2.99	0.0060	0.20	1.14	2.55	2.23	305.28	-	314.9	305.5
1.2.3	6/17/2004	13:00	4.58	1.15	0.44	2.00	0.56	0.46	3.00	0.0063	0.21	1.14	2.55	2.23	305.31	-	317.0	305.8
1.3.1	6/17/2004	16:15	4.63	1.16	0.47	2.00	0.29	0.24	3.14	0.0177	0.56	1.14	5.12	4.50	306.52	-	314.7	311.8
1.3.2	6/17/2004	16:45	4.64	1.16	0.49	2.00	0.13	0.22	2.87	0.0250	0.87	1.14	5.13	4.51	306.56	-	314.1	311.4
1.3.3	6/17/2004	17:45	4.66	1.16	0.48	2.00	0.28	0.24	3.18	0.0284	0.89	1.14	5.12	4.50	306.55	-	313.7	311.5
1.4.1	6/17/2004	18:30	4.68	1.17	0.49	2.00	0.34	0.39	5.04	0.0352	0.70	1.15	5.12	4.44	305.43	-	313.2	312.5
1.5.1	6/17/2004	19:15	4.67	1.17	0.50	2.00	0.21	0.31	4.01	0.0388	0.97	1.15	5.10	4.43	304.65	-	313.3	311.8
1.6.1	6/18/2004	15:30	4.67	1.17	0.47	2.00	0.52	0.66	11.34	0.3153	2.78	0.71	3.95	5.57	306.56	-	312.6	317.3
1.7.1	6/21/2004	16:45	4.63	1.15	0.49	2.02	0.58	0.66	11.49	0.7318	6.37	0.48	2.58	5.41	305.38	315.44	313.7	312.4
Removed Water																		
1.8.1	6/22/2004	17:45	5.66	1.40	0.46	2.05	0.86	0.90	3.29	0.2171	6.60	2.25	2.67	1.19	310.55	316.58	314.23	302.95
1.8.2	6/22/2004	18:30	5.62	1.39	0.47	2.05	0.47	0.92	3.37	0.2348	6.97	2.25	2.66	1.18	310.74	316.41	314.60	302.56
1.9.1	6/22/2004	19:30	5.59	1.38	0.47	2.05	0.73	1.15	3.50	0.4569	13.06	2.91	2.66	0.92	319.97	314.94	314.61	304.77
1.9.2	6/22/2004	20:15	5.60	1.38	0.48	2.05	0.56	1.15	3.55	0.4879	13.74	2.91	2.68	0.92	319.53	315.03	314.70	304.66
1.10.1	6/22/2004	21:15	5.63	1.39	0.49	2.05	0.42	0.58	2.95	0.0552	1.87	1.54	2.69	1.75	301.96	315.69	314.72	303.41
1.10.2	6/22/2004	22:00	5.63	1.39	0.48	2.05	0.55	0.53	2.66	0.0428	1.61	1.54	2.63	1.71	300.90	315.89	314.70	303.02
1.11.1	6/23/2004	8:15	5.74	1.42	0.48	2.05	0.69	0.74	2.67	0.2234	8.35	1.17	1.34	1.14	296.69	308.95	307.83	295.81
1.11.2	6/23/2004	9:00	5.71	1.41	0.50	2.05	0.49	0.72	2.45	0.1802	7.35	1.17	1.29	1.10	297.08	309.11	308.38	295.73
1.12.1	6/23/2004	14:30	5.71	1.41	0.51	2.05	0.40	0.49	2.10	0.3318	15.79	2.98	3.73	1.25	325.69	315.87	312.95	307.50
1.12.2	6/23/2004	15:15	5.71	1.41	0.59	2.05		0.62	2.62	0.3975	15.19	2.99	3.75	1.25	325.66	316.63	312.86	307.62
1.13.1	6/23/2004	17:30	5.71	1.41	0.52	2.05	0.51	1.16	13.21	1.1900	9.01	1.21	4.10	3.39	303.75	323.09	313.61	311.72
1.14.1	6/23/2004	18:15	5.73	1.41	0.54	2.05	0.61	0.92	12.66	1.1599	9.16	1.01	4.13	4.10	303.02	323.00	313.49	314.02
1.15.1	6/24/2004	9:00	5.85	1.45	0.52	2.05	0.51	0.86	11.90	1.3153	11.05	1.02	4.16	4.07	297.74	306.73	311.26	312.14
1.15.2	6/24/2004	9:30	5.79	1.43	0.53	2.05	0.55	0.83	11.10	0.9200	8.29	1.01	4.15	4.09	298.56	315.52	315.66	313.88
1.16.1	6/24/2004	10:30	5.73	1.42	0.54	2.05	0.56	0.96	11.64	1.6946	14.56	1.21	4.17	3.44	300.16	324.49	316.80	311.59
1.16.2	6/24/2004	11:00	5.75	1.42	0.54	2.05	0.56	0.99	11.97	1.6582	13.85	1.21	4.15	3.44	301.63	323.09	315.81	311.93
1.17.1	6/24/2004	12:15	5.77	1.43	0.54	2.05	0.51	0.83	11.18	0.7531	6.74	0.65	2.68	4.15	299.92	321.69	314.57	311.42
1.17.2	6/24/2004	12:30	5.84	1.44	0.54	2.05	0.53	0.85	11.17	0.5822	5.21	0.65	2.67	4.14	299.90	321.11	314.41	311.59
Removed Water																		
1.18.1	6/24/2004	16:00	6.11	1.54	0.53	1.97	0.73	0.89	11.80	0.4309	3.65	0.99	4.20	4.25	306.40	325.99	319.50	316.20
1.18.2	6/24/2004	16:15	6.19	1.54	0.52	2.01	0.76	0.91	12.04	0.4309	3.58	0.99	4.17	4.21	307.16	326.21	319.27	316.74
1.19.1	6/24/2004	17:00	6.20	1.55	0.53	2.01	0.66	0.83	11.15	0.5783	5.18	0.64	2.70	4.24	306.27	327.13	318.54	314.06
1.19.2	6/24/2004	17:30	6.15	1.52	0.53	2.05	0.67	0.84	11.29	0.4524	4.01	0.64	2.71	4.27	305.31	325.94	318.27	313.02

1. Loading: mol CO_2/Total Alkalinity
2. Penetration: CO_2 Out/CO_2 In
3. Estimated values shown by italics
4. Define as mol/kg of solution

47

Titrations and ICP analyses were performed only at the beginning and end of each concentration change. The piperazine and potassium concentrations in between the runs were back-calculated from density measurements. The data showed a strong correlation between potassium concentration and density measurements. Therefore, the density measurements were used to determine a potassium concentration. It was assumed that the piperazine to potassium concentration remained relatively unchanged. Thus, the piperazine to potassium ratio was calculated as the average of the beginning and end ratios. The piperazine concentration was then back-calculated based on this average ratio.

In Run 1.1.1, the concentration of potassium carbonate was slightly low. Therefore, an additional ¾ drum of potassium carbonate was added to the system. In Runs 1.2.1 through 1.7.1, the potassium to piperazine concentration was determined to be approximately 2:1. The table shows that the results for piperazine concentration from titration and the TOC analysis are comparable. However, the results for potassium from the ICP analysis differed from the titration analysis between 3 to 35%.

For Runs 1.8.1 to 1.17.2, 5 drums of condensate were removed to further concentrate the solvent system. The potassium concentration appeared to have slightly changed. This may have been due to operations with an increased level in the liquid accumulator. In the final set of runs, an additional drum of condensate was removed and the liquid accumulator was operated with a higher liquid level. The column was not operated on a continuous 24-hour basis as originally planned due to the numerous problems that were encountered. The condensate did not contain appreciable amounts of piperazine (Table 9). Total alkalinity ranged from 0.07 to 0.13 mol/kg solution.

Table 9. Total Alkalinity for Stripper Condensate

Sample ID	Total Alkalinity mol/kg soln
Barrel 1	0.07
Barrel 2	0.08
Barrel 3	0.13
Barrel 4	0.09
Barrel 5	0.08

A total of 5 absorber temperature profiles were acquired using a thermal imaging gun. The results indicate that a large bulge occurred towards the top of the column and at the spool piece, a large temperature gradient also exists. A minor temperature bulge also appears in the bottom section of the column. The temperature bulge occurs where most of the mass transfer takes place because the heat of CO_2 absorption is fairly large.

Corrosion coupons were inserted into a 2-inch pipe just downstream of the feed heater and left in the system over a 1 week period. A total of 11 coupons were inserted. The materials that were tested include 304L (Stainless Steel - SS), 316L (SS), 2205 (Duplex), 1010 (Carbon

Steel), 317L (Stainless Steel), and fiber reinforced plastic (FRP). Each coupon was weighed at the beginning and end of the week-long run. Preliminary results show that all of the steel coupons remained relatively unchanged. However, the FRP seemed to have absorbed some of the solvent, as the final weight seemed to be a little higher.

The product of the gas flowrate and the natural log of penetration are plotted against the liquid flowrate (Figure 19). The top set of data represent data at 3% CO_2 and the bottom set at 12% CO_2. At a given inlet CO_2 concentration, the penetration appears to be inversely proportional to the gas rate. Performance with 3% CO_2 was substantially better than at 12% CO_2. With 3% inlet CO_2, the product of gas flow and natural log of penetration was about 6 kg/m^2-s. The penetration varied from 0.2 to 15.8%. Two outlying 3% points at the low liquid rates represent data taken at low inlet gas and liquid temperatures. Also, both the gas and liquid rates are low. It may be that at these low gas and liquid rates, the packing is not adequately wetted and hence the performance suffers.

Table 10. Corrosion Coupon Results

Sample ID	Mass Before g	Mass After G	Difference
C1010-1	15.6816	15.6824	-0.0008
C1010-2	15.8699	15.8705	-0.0006
304L-1	14.6760	14.6762	-0.0002
304L-2	14.7226	14.7232	-0.0006
316L-1	14.3783	14.3791	-0.0008
316L-2	14.3493	14.3496	-0.0003
317L-1	14.7838	14.7839	-0.0001
317L-2	14.7172	14.7179	-0.0007
2205-1	15.1899	15.1903	-0.0004
2205-2	15.3256	15.3267	-0.0011
FRP	10.4145	10.4408	-0.0263

The liquid CO_2 capacity measurements did not match the gas phase CO_2 capacity calculated by a material balance. It is possible that the liquid analysis may have some type of systematic error. It is also possible that the gas-phase measurements were not completely accurate. At low L/G ratios, the liquid outlet temperature approaches the temperature of the inlet gas. At high L/G ratios, the liquid outlet temperature is 10 to 15 degrees higher than the inlet gas temperature.
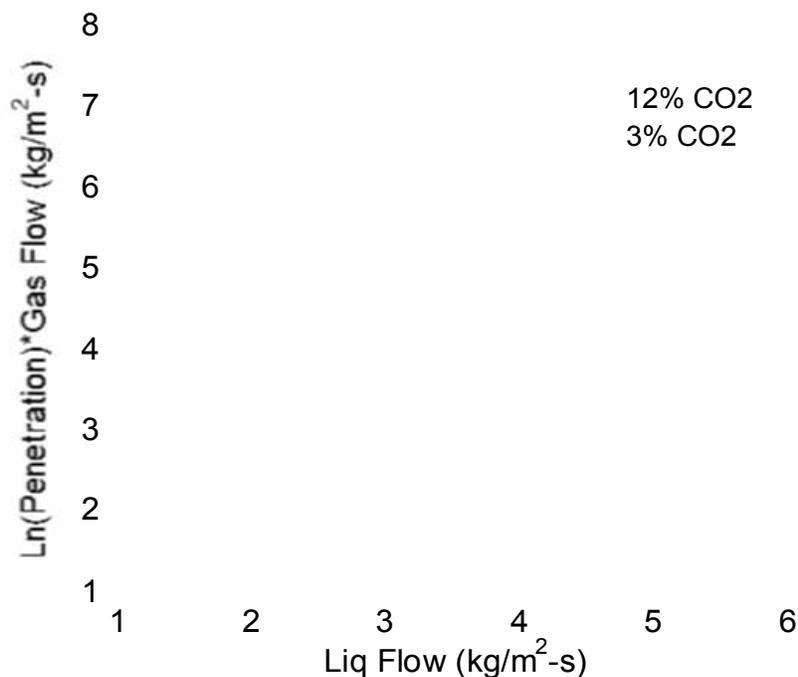
Figure 19. Absorber Performance for 3% and 12% CO$_2$

Conclusions and Future Work

The penetration with 3% CO$_2$ varied from 0.2% at a gas rate of 1.14 kg/m^2-s to 15.8% at 3.0 kg/m^2-s. CO$_2$ penetration with 12% CO$_2$ varied from 3.0% at a gas rate of 0.7 kg/m^2-s to 15.0% at 1.2 kg/m^2-s. Neither the dissolved iron concentration nor the corrosion coupons suggest any significant corrosion occurred with 1000 ppm vanadium during the short term campaign. The pilot plant was operated at 3 and 12 % CO$_2$ and the gas and liquid rates varied from 0.5 to 3.0 kg/m^2-s and 1.3 to 5.1 kg/m^2-s, respectively. At 12% CO$_2$, the maximum gas rate was limited by the stripper. The gas cooler temperature control will be corrected and the steam traps for the solvent preheater will be replaced before the start of the next campaign. Campaign 2 is scheduled to begin in late September.

Further data analysis will be done and additional correlations developed. The model will be modified to fit the data obtained from the pilot plant experiments. The VLE and k$_g$' models used in the adiabatic absorber model will be improved to better fit the data. The model will be modified to the fit the effective area data obtained from the CO$_2$/KOH absorption data. A new and more efficient convergence algorithm will be also implemented and other mass transfer and pressure drop models will be added.

References

Al-Juaied, M, "Carbon Dioxide Removal from Natural Gas by Membranes in the Presence of Heavy Hydrocarbons and by Aqueous Diglycolamine®/Morpholine," Ph.D. Dissertation, The University of Texas at Austin (2004).

Aseyev, G. G., and I. D. Zaytsev [translated from Russian by Yu. A. Gorshkov.], *Volumetric Properties of Electrolyte Solutions: Estimation Methods and Experimental Data*, Begell House, New York (1996).

Aseyev, G. G., *Electrolytes: Equilibria in Solutions and Phase Equilibria. Calculation of Multicomponent Systems and Experimental Data on the Activities of Water, Vapor Pressures, and Osmotic Coefficients*, Begell House, New York (1999).

Astarita, G., D. W. Savage, and A. Bisio, *Gas Treating with Chemical Solvents*, Wiley & Sons, New York (1983).

Austgen, D. M., "A Model of Vapor-Liquid Equilibria for Acid Gas-Alkanolamine-Water Systems," Ph.D. Dissertation, The University of Texas at Austin (1989).

Bishnoi, S., "Carbon Dioxide Absorption and Solution Equilibrium in Piperazine Activated Methyldiethanolamine," Ph.D. Dissertation, The University of Texas at Austin (2000).

Britt, H. I., and R. H. Luecke, "The Estimation of Parameters in Nonlinear, Implicit Models," *Technometrics*, **15**(2), 223- 247 (1973).

Caplow, M., "Kinetics of Carbamate Formation and Breakdown," *J. Am. Chem. Soc.* **90**(24), 6795-6803 (1963).

Caracotsios, M., "Model Parametric Sensitivity Analysis and Nonlinear Parameter Estimation. Theory and Applications," Ph.D. Dissertation, University of Wisconsin (1986).

Chen, C. C., H. I. Britt, J. F. Boston, and L. B. Evans, "Local Composition Model for Excess Gibbs Energy of Electrolyte Systems. Part I: Single Solvent, Single Completely Dissociated Electrolyte Systems," *AIChE J.,* **28**(4), 588-96 (1982).

Chen, C.-C., H. I. Britt, J. F. Boston, and L. B. Evans, "Extension and Application of the Pitzer Equation for Vapor-Liquid Equilibrium of Aqueous Electrolyte Systems with Molecular Solutes," *AIChE J.*, **25**(5), 820-31 (1979).

Cullinane, J. T., "Carbon Dioxide Absorption in Aqueous Mixtures of Potassium Carbonate and Piperazine," M.S. Thesis, Department of Chemical Engineering, The University of Texas at Austin (2002).

Cullinane, J. T., and G. T. Rochelle, "Equilibrium Behavior of Aqueous Potassium Carbonate, Piperazine, and Carbon Dioxide," in preparation for submission to *Fluid Phase Equilibria* (2004).

Cullinane, J.T., B. A. Oyenekan, J. Lu, and G. T. Rochelle,. "Aqueous Piperazine/Potassium Carbonate for Enhanced CO_2 Capture," to be presented at GHGT-7, Vancouver, Canada (2004).

Edwards, T. J., G. Maurer, J. Newman and J. M. Prausnitz, "Vapor-Liquid Equilibria in Multicomponent Aqueous Solution of Volatile Weak Electrolytes," *AIChE J.,* **24**(6), 966-976 (1978).

Ermatchkov, V., A. P.-S. Kamps, and G. Maurer, "Chemical Equilibrium Constants for the Formation of Carbamates in (CO2+Piperazine+Water) From 1H-NMR Spectroscopy," *J. Chem. Thermodyn.* **35**(8), 1277-1289, (2003).

Freguia, S., "Modeling of CO_2 Removal from Flue Gases with Monoethanolamine," M.S. Thesis, Department of Chemical Engineering, The University of Texas at Austin (2002).

Glasscock, D., "Modeling and Experimental Study of Carbon Dioxide Absorption into Aqueous Alkanolamines," Ph.D. Dissertation, The University of Texas at Austin (1990).

Gmehling, J., J. Li, and M. Schiller, "A Modified UNIFAC Model. 2. Present Parameter Matrix and Results for Different Thermodynamic Properties," *Ind. & Eng. Chem. Res.*, **32**(1), 178-93 (1993).

Hetzer, H. B., R. A. Robinson, and R. G. Bates, "Dissociation Constants of Piperazinium Ion and Related Thermodynamic Quantities from 0 to 50.Deg.," *J. Phys. Chem.,* **72**(6), 2081-6 (1968).

Inventory of U.S. Greenhouse Gas Emissions and Sinks: 1990-2000, U.S. Environmental Protection Agency, Office of Atmospheric Programs, EPA 430-R-02-003, April 2002. Available at:: http://www.epa.gov/globalwarming/publications/emissions.

Jou, F.Y., and A. E. Mather, "The Solubility of CO_2 in a 30 Mass Percent Monoethanolamine Solution," *Can. J. Chem. Eng.*, **73**(1), 140-7 (1995).

Kamps, A. P., J. Xia, and G. Maurer, "Solubility of CO_2 in (H_2O + Piperazine) and in (H_2O + MDEA + Piperazine)," *AIChE J.,* **49**(10), 2662-2670 (2003).

Oyenekan, B. A., and G. T. Rochelle, "Stripper Models for CO_2 Capture by Aqueous Solvents," to be presented at GHGT-7, Vancouver Canada (2004).

Pacheco, M. A., "Mass Transfer, Kinetics and Rate-Based Modeling of Reactive Absorption," Ph.D. Dissertation, The University of Texas at Austin (1998).

Posey, M. L., "Thermodynamic Model for Acid Gas Loaded Aqueous Alkanolamine Solutions," Ph.D. Dissertation, The University of Texas at Austin (1996).

Renon, H., and J. M. Prausnitz, "Local Compositions in Thermodynamic Excess Functions for Liquid Mixtures," *AIChE J.,* **14**(1), 135-44 (1968).

Roy, R. N., J. J. Gibbons, R. Williams, L. Godwin, G. Baker, J. M. Simonson, and K. S. Pitzer, "The Thermodynamics of Aqueous Carbonate Solutions. I. Mixtures of Potassium Carbonate, Bicarbonate, and Chloride," *J. Chem. Thermodyn.*, **16**(4), 303-15 (1984).

Sarbar, M., A. K. Covington, R. L. Nuttall, and R. N. Goldberg, "Activity and Osmotic Coefficients of Aqueous Potassium Carbonate," *J. Chem. Thermodyn.*, **14**(7), 695-702 (1982).

Tosh, J. S., J. H. Field, H. E. Benson, and W. P. Haynes, "Equilibrium Study of the System Potassium Carbonate, Potassium Bicarbonate, Carbon Dioxide, and Water," U.S. Bur. Mines, Rept. Invest. No. 5484, 23 pp (1959).

Versteeg, G. F., and W. P. M. Van Swaaij, "Solubility and Diffusivity of Acid Gases (CO_2, N_2O) in Aqueous Alkanolamine Solutions," *J. Chem. Eng. Data,* **33**(1), 29-34 (1988).

Wilson, I., "Gas-Liquid Contact Area of Random and Structured Packing," M.S. Thesis, Department of Chemical Engineering, The University of Texas at Austin (2004).